THE INFLUENCE OF NONCIRCULAR CHAINRINGS ON MAXIMAL AND SUBMAXIMAL CYCLING PERFORMANCE

by

Chee Hoi Leong

A dissertation submitted to the faculty of
The University of Utah,
in partial fulfillment of the requirements for the degree of

Doctor of Philosophy

Department of Exercise and Sport Science

The University of Utah

December 2014

The University of Utah Graduate School

STATEMENT OF DISSERTATION APPROVAL

The dissertation of **Chee Hoi Leong**

has been approved by the following supervisory committee members:

James C. Martin	, Chair	**07/25/2014** Date Approved
Charlie A. Hicks-Little	, Member	**07/23/2014** Date Approved
Bruce A. MacWilliams	, Member	Date Approved
William J. McDermott	, Member	Date Approved
Steven J. Elmer	, Member	**07/17/2014** Date Approved

and by **James C. Hannon** , Chair of the Department of **Exercise and Sport Science**

and by David B. Kieda, Dean of The Graduate School.

ABSTRACT

Most cycling power is produced during leg extension with minimal power production occuring during the transition between the extension-flexion phases. A prolonged leg extension phase and reduced transition phase could increase cycling power by allowing muscles to generate power for a greater portion of the cycle. Noncircular chainrings have been designed to prolong the time spent in the powerful leg extension phase by varying crank angular velocity within the pedal cycle. The purposes of this dissertation were to evaluate the extent to which noncircular chainrings influence power, biomechanics, and metabolic cost during maximal and submaximal cycling. In the first study, I investigated the effects of chainring eccentricity (C = 1.0, R = 1.13, O = 1.24) on maximum cycling power (P_{max}) and optimal pedaling rate (RPM_{opt}). Chainring eccentricity did not influence P_{max} and RPM_{opt}. Despite reasonable theory regarding a prolonged leg extension phase and reduced transition phase, chainring eccentricity did not influence P_{max} and RPM_{opt} during maximal cycling. In the second study, I evaluated the influence of noncircular chainrings on joint-specific kinematics and power production during maximal cycling. Ankle angular velocity was significantly reduced (-13±12% and -37±13% at 90 and 120 rpm, respectively) with the O chainring, whereas knee and hip angular velocities were unaffected during the leg extension phase. Further, joint-specific power production was unaffected by chainring eccentricity. These results demonstrate that redundant degrees of freedom (DOF) in the cycling action (i.e., ankle angle) allowed

cyclists to negate the effects of eccentricity and maintain their preferred hip and knee actions. In my third study, I evaluated the extent to which chainring eccentricity influenced metabolic cost and biomechanics of submaximal cycling. My study protocol allowed for separate analysis of eccentricity and pedal speed (known to influence metabolic cost). Chainring eccentricity with similarly matched pedal speeds reduced knee (-10%) and hip (-5%) angular velocities, while metabolic cost and cycling efficiency remained unaffected. Despite small but significant alterations in joint-specific kinematics, chainring eccentricity did not influence metabolic cost or cycling efficiency during submaximal cycling. Taken together, these results indicate that commercially available noncircular chainrings do not provide performance benefits over conventional circular chainrings during maximal and submaximal cycling.

TABLE OF CONTENTS

LIST OF TABLES

LIST OF FIGURES

ACKNOWLEDGEMENTS

This dissertation has been made possible by the contributions of many people who have helped and supported me in the completion of this project. Dr. James Martin, you are an exceptional mentor, confidante, colleague, and friend. Thank you for providing me with the opportunities to develop as a scholar and researcher under your tutorage.

I would also like to sincerely thank my dissertation committee of Charlie Hicks-Little, Bruce MacWilliams, William McDermott, and Steven Elmer for their guidance, support, and encouragement throughout my dissertation. In addition, I would like to acknowledge Dr. Rick Neptune for providing his insightful comments during discussions with our Neuromuscular Function Laboratory group leading to the conception of the methodologies.

Most importantly, great appreciation goes to my wife, Tan Leng. Thank you for going through this entire academic journey with me, by giving me your patience, support, and love. Thank you for taking care of our newborn, Gavin, during the final months of this project, affording me the time and focus to complete the final stages of this project.

On a final note, I want to express a heartfelt thanks to the participants who volunteered in these series of studies and the students in the Neuromuscular Function Laboratory for their assistance with data collection.

CHAPTER 1

INTRODUCTION

During maximal cycling, muscular power performed during whole-leg extension occurring between the crank angles of 333° to 165° accounts for 80% of net cycling power (14, 24), where cranks angles of 0° and 360° represent the top dead center of the pedal position. Previous investigators have sought to increase maximal cycling power with various strategies involving the manipulation of pedaling motion, such as pedaling rate, crank length, the use of novel crank-pedal mechanisms, and noncircular chainrings (19, 20, 32, 34, 36). During cycling with standard circular chainrings, crank angular velocity is relatively constant throughout the pedal cycle. Noncircular chainrings alter the time spent in each portion/section of the pedal cycle by varying the gear ratio and hence the crank angular velocity within the pedal cycle. Consequently, a noncircular chainring can be designed to increase the time spent in the leg extension and flexion phases, where powers are high, while reducing the time spent in the transition phase, where power is low (14). This strategy of manipulating the instantaneous crank angular velocity may provide a strategy for maximizing cycling power within the pedal cycle.

Eccentricity is the measure of an ellipse/conic section's deviation from the shape of a circle (Figure 1.1) defined as the ratio of major-to-minor axes, where *a* is the length

of the major axis and *b* is the length of the minor axis. The degree of variation in crank angular velocity in a noncircular chainring is determined by its degree of eccentricity. Noncircular chainrings introduce variations in crank angular velocity relative to a circular chainring, thus altering the time spent in the leg extension and flexion phases of the pedal cycle. Noncircular chainring manufacturers (e.g., Rotor and Osymetric) claim that a noncircular chainring shape could increase the time spent in the leg extension and flexion phases, where powers are high, and reduce the time spent in the transition phase, where power is low. Hence, this strategy of manipulating the instantaneous crank angular velocity may provide a strategy for increasing maximal cycling power averaged over a complete pedal cycle.

Previous investigations evaluating the influence of chainring eccentricity on maximal cycling power have produced mixed results. Some investigators reported increases (32, 34), while others reported no improvements in maximal cycling power (16, 33). Rankin and Neptune (34) performed a theoretical analysis of noncircular chainrings and suggested that an elliptical chainring of average eccentricity of 1.29 can increase maximum cycling power by approximately 3% over a range of pedaling rates (60, 90, and 120 rpm). These authors matched the pedaling rate for the chainring conditions. Thus, it would have involved power production at different pedal speeds (product of pedaling rate and chainring radius), resulting in lower speeds for the noncircular chainrings. Because pedal speed is known to influence joint angular velocity and therefore muscle shortening velocity (24, 25), these observations of increased power at similar pedaling rates may have biased the effect of chainring shape by not seeking out the optimal pedaling rate for each chainring condition. Hence, in the first study I evaluated the influence of

noncircular chainrings of different eccentricities (1.15 and 1.24) on maximum cycling power and the maximal power-pedaling rate relationship (including optimal pedaling rate).

The degree to which instantaneous crank angular velocity will influence muscle and joint actions depends on the degrees of freedom (DOF) in the leg, crank, pedal system. If the hip joint were fixed and the ankle joint center rotated about the pedal spindle, then the leg/crank/pedal system would have a single DOF and crank angular velocity would completely determine hip and knee joint angular velocities. The theoretical analysis of noncircular chainring shape by Rankin and Neptune (34) involving three rotational DOF (crank and two pedal angles) demonstrated an increase in maximum cycling power by approximately 3% over a range of pedaling rates (60, 90, and 120 rpm). However, movement of the hip joint center and angular movement of the ankle represent additional DOF in the system. These additional DOF allow the cyclist to manipulate joint angular velocity with substantial independence from crank angular velocity and potentially negate the effects of the noncircular chainring. Indeed, Shan (37) reported significant changes in ankle kinematics with unchanged knee and hip kinematics while pedaling with a noncircular crank system (37). Further, Martin and Brown (24) reported that cyclists exploited redundant degrees of freedom during cycling action to increase the time for ankle, knee, and hip extension. Thus, in the second investigation, I evaluated the effects of noncircular chainrings on cycling power and joint biomechanics (joint-specific kinematics and powers) during maximal cycling.

The manipulation of instantaneous crank angular velocity with a noncircular chainring shape may allow for whole-leg extension action to act for a greater portion of

the time within a pedal cycle thus increasing net cycling power. In addition, a noncircular chainring shape reduces the time spent in the two the transition areas between extension and flexion. However, reducing time spent in extension-flexion transition phases may require an increase in energy expenditure because moving more quickly through the transitions requires greater kinetic energy (22). Indeed, findings on physiological responses during submaximal cycling with the use of noncircular chainrings have been mixed. Some previous investigators reported reductions in blood lactate concentration, and metabolic cost with concomitant increases in average cycling power with the use of noncircular chainrings over conventional circular chainrings (15, 32). In contrast, several other investigators detected no physiological effects between circular and noncircular chainrings (18, 20, 33, 35). Another plausible explanation for the mixed findings of chainring shape/eccentricity on submaximal cycling performance could be the lack in the control of pedaling rate. Because pedaling rate influences both cycling efficiency and metabolic cost (5, 9), the lack of control of pedaling rate may have contributed to these mixed findings. Therefore, in my final investigation, I evaluated cycling biomechanics and the metabolic cost of producing submaximal cycling power with circular and noncircular chainrings. My protocol controlled pedaling rate as well as pedal speed during leg extension (where the majority of power is produced). Thus, my design decoupled pedaling rate from chainring shape/eccentricity by determining the separate contributions of pedaling rate and chainring shape/eccentricity. Collectively, the results from these studies may have implications for researchers, clinicians, equipment manufacturers, as well as coaches and athletes, considering the use of specialized equipment with the potential to improve cycling performance. In the subsequent chapters

of this dissertation (Chapters 2, 3, and 4), I discuss each of these studies in detail and provide an overall summary, implications, and recommendations for future directions in the final chapter (Chapter 5).

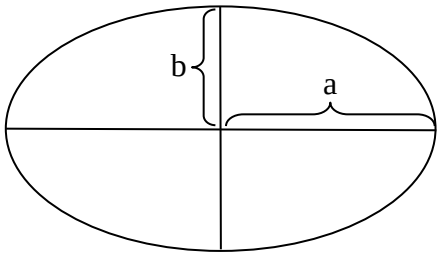

Figure 1.1: Schematic of an ellipse. An ellipse with eccentricity defined as the ratio of major-to-minor axes, where *a* is the length of the major axis and *b* is the length of the minor axis.

CHAPTER 2

EFFECTS OF NONCIRCULAR CHAINRINGS ON MAXIMUM CYCLING POWER AND OPTIMAL PEDALING RATE

During cycling, muscular power is produced during both leg extension and flexion actions (14, 24). In contrast, very little power is produced during the transition between leg extension and flexion. Standard circular chainring produces a relatively constant angular velocity throughout the pedal cycle. Alternatively, a noncircular chainring profile varies crank angular velocity within the pedal cycle. Variable crank angular velocity can alter the time spent in each portion/section of the pedal cycle. For example, it could increase the time spent in the leg extension and flexion phases, where powers are high, and reduce the time spent in the transition phase, where power is low (14, 20, 28).

Two previous investigators have evaluated the effects of noncircular chainrings on maximal cycling power. O'Hara and colleagues (32) reported a 6% significant increase in average power in a 1km time trial with Rotor Q-Rings over circular chainrings. These authors allowed participants to self-select their preferred gear ratios for the two conditions, indicating that pedaling rates may not have been matched. Pedaling rate governs two distinct physiological phenomena of 1) frequency of muscle activation and relaxation, and 2) muscle shortening velocity (25, 40). Thus, in this study

design the increase in cycling power with the use of the Rotor Q-Rings may have been due to a pedaling rate effect, as opposed to a chainring/eccentricity effect. Rankin and Neptune (34) performed a theoretical analysis of noncircular chainrings and determined that an elliptical chainring of average eccentricity of 1.29 would increase maximum cycling power by approximately 3% over a range of pedaling rates (60, 90, and 120 rpm). This observation of increased power at similar pedaling rates is interesting. While the larger chainring radii encountered during the leg extension phase might be to increase the time spent during the extension action, it would also reduce the instantaneous pedal speed. Pedal speed is known to influence joint angular velocity and therefore muscle shortening velocity (23, 40). Thus, cycling at similar pedaling rates involved power production at different pedal speeds: lower speeds for the noncircular chainrings. Consequently, Rankin and Neptune (34) may have underreported the beneficial effects of noncircular chainrings. Hence, the purpose of this study was to expand upon the work of these previous investigators by evaluating the influence of different chainring eccentricities on the power-pedaling rate relationship during maximal cycling. The parabolic shape of the power-pedaling rate relationship allows the identification of maximum cycling power (P_{max}), and the pedaling rate at which P_{max} occurred, defined as optimal pedaling rate (RPM_{opt}). Additionally, the power-pedaling rate relationship allows cycling power to be evaluated across a range of pedaling rates. Hence, a shift in the power-pedaling rate relationship would likely indicate the influence of chainring eccentricity on cycling power across a range pedaling rates. I hypothesized that a chainring with greater eccentricity would facilitate greater power production than a chainring with less eccentricity. In addition, a chainring with greater eccentricity would

also facilitate the production of P_{max} at lower RPM_{opt}.

Methods

Participants

Thirteen trained cyclists (12 males and 1 female) licensed as category 3 or 4 by USA Cycling volunteered to participate in this investigation (participant characteristics are presented in Table 2.1). None of the participants had previous experience in using noncircular chainrings. Experimental procedures used in this investigation were reviewed and approved by the University of Utah Institutional Review Board (IRB_00029248). The protocol and procedures were explained verbally, and all participants provided written informed consent prior to testing. Participants reported to the laboratory prior to the experimental days in order to become familiarized with the maximal cycling trials (described below). Briefly, participants performed three familiarization sessions of maximal cycling trials the week before the actual data collection. The cycle ergometer was configured such that participants were blinded to each chainring eccentricity: standard circular (C, eccentricity = 1.0), Rotor (R, eccentricity = 1.13), and Osymetric (O, eccentricity = 1.24). Because participants could sense differences in the pedaling action, they were asked to provide their perception of the chainring used for the cycling trials at the end of each testing session. The ergometer seat height was adjusted to match each participant's accustomed cycling position.

Experimental Protocol

Prior to the week of experimental data collection, participants performed three familiarization sessions with each chainring eccentricity. During each of the three familiarization sessions, participants performed a 5 min warm-up of steady state cycling (100-150W, 90 rpm) using one of the three randomly assigned chainring eccentricities. Participants then performed three maximal power trials (4 s) with 2 min of recovery between trials. The same procedures were employed during the experimental data collection week.

Chainring Conditions

The cycle ergometer was configured with chainring conditions of eccentricities (ratio of major-to-minor axes) 1.0, 1.13, and 1.24, using a conventional 53 tooth circular (C) chainring, a 53 tooth Rotor Q-Ring (R), and a 54 tooth Osymetric (O) chainring, respectively. The shape of the R chainring (Rotor BIKE USA, Colorado Springs, CO, USA) is described as an ellipse where the major and minor axes are perpendicular (Figure 2.1A). The shape of the O chainring (Osymetric USA, Winston-Salem, NC, USA) is described as a skewed ellipse where the major and minor axes are not perpendicular, with the major oriented at 73° forward of the minor axis (Figure 2.1B). Because the R and O chainrings have been designed to prolong the time spent in the leg extension phase, the crank arms for the R and O chainrings were oriented such that the smallest chainring radii are encountered (minor axes) at the beginning of leg extension during maximal cycling. More precisely, the radii of the R and O chainrings progressively increased, reaching their maximum within the complete whole leg extension range of 333° to 165° typically

observed with a C chainring (14). Consequently, the R crank arm was oriented at 61° forward of the major axis and 29° behind the minor axis (Figure 2.1A), and the O crank arm was oriented at 71° forward of the major axis and 36° behind the minor axis (Figure 2.1B).

Maximal Cycling Power (P_{max})

Participants performed three maximal cycling trials on an inertial-load cycle ergometer (29). The inertial-load method determined cycling power across a range of pedaling rates (e.g., 60-180 rpm) in a single brief trial and has been previously described by Martin and colleagues (29). These cycling trials were of short duration, each lasting approximately 3-4 s, and thus did not elicit fatigue or pronounced pain in the legs. The ergometer was fitted with racing handlebars, cranks, saddle, and fixed to the floor. Participants wore cycling shoes that locked onto the pedal (Speedplay Inc., San Diego, CA, USA). Following a 5-min cycling warm-up (100-150 W), participants began each trial from rest and accelerated maximally for eight pedal revolutions with resistance provided solely by the moment of inertia of the flywheel. Participants were instructed to remain seated throughout each trial and were given standardized verbal encouragement. Flywheel angular position data were low pass filtered at 8 Hz using a 5th order spline routine (39) and velocity and acceleration were determined from the spline coefficients. Power averaged over each complete crank revolution was calculated as rate of change in kinetic energy and maximum power was identified as the apex of the power-pedaling rate relationship. Maximum cycling power (P_{max}) values were averaged for the three trials at each time point. The pedaling rate at which P_{max} occurred was defined as optimal

pedaling rate (RPM_{opt}). Following the three trials, participants were allowed to cycle at low intensity (cool down) as long as they wish. Note that it has been reported that active individuals require two days of practice in order to produce valid and reliable power values (26). In an effort to reduce the influence of motor learning, participants performed three days of maximal cycling familiarization trials. Thus, the participants were adept at the cycling technique used in this investigation and able to produce reliable values for maximal cycling power.

Data Analysis

A one-way repeated measures analysis of variance (ANOVA) was used to evaluate P_{max} , RPM_{opt}, and chainring perception across the different chainring conditions. In addition, cycling powers at pedaling rates of 90, 120, and 150 rpm were interpolated from the power-pedaling rate relationships for each chainring condition. A two-way (pedaling rate × eccentricity) repeated measures ANOVA was used to evaluate cycling powers at pedaling rates of 90, 120, and 150 rpm across the different chainring conditions. If any of the ANOVA procedures indicated a significant main effect or significant interaction, pair-wise comparisons (Fisher's least significant differences) were used to determine where differences occurred. Values are reported as mean±standard error of the mean (SEM), and alpha was set at 0.05.

Results

Maximum cycling powers (P_{max}) produced for the C (1157±273 W), R (1148±259 W), and O (1127±250 W) chainring conditions were not significantly different (p = 0.15;

Table 2.2). Similarly, the optimal pedaling rates (RPM_{opt}) for the C (126±13 rpm), R (123±9 rpm), and O (122±14 rpm) chainring conditions did not differ ($p = 0.19$; Table 2.2). The repeated measures ANOVA revealed a significant pedaling rate × eccentricity interaction ($p < 0.05$) on the cycling powers at pedaling rates of 90, 120, and 150 rpm interpolated from the power-pedaling rate relationships for each chainring condition. Subsequent post hoc analyses indicated that interpolated power produced at 150 rpm differed between the C (1054±287 W) and O (995±271 W) chainring conditions ($p < 0.05$; Figure 2.2). In contrast, interpolated power produced at 90 rpm for C (998±188 W), R (1003±187 W), and O (996±190 W) chainring conditions did not differ ($p = 0.73$; Figure 2.2). Similarly, interpolated power produced at 120 rpm for C (1125±253 W), R (1120±243 W), and O (1097±243 W) chainring conditions were not significantly different ($p = 0.08$; Figure 2.2). The power-pedaling rate relationships for each chainring condition are shown in Figure 2.2B.

Participants achieved 46±14%, 31±13%, and 92±8% accuracy in chainring perception for the C, R, and O chainring conditions, respectively. Repeated measures ANOVA revealed that participants achieved the greatest perceptual accuracy with the O compared to the C and R chainring conditions (both $p < 0.01$). In contrast, there was no significant difference in chainring perception between the C and R chainring conditions ($p = 0.44$). In other words, these experienced cyclists were unable to distinguish C from R chainring condition.

Discussion

Theoretically, noncircular chainrings can potentially increase cycling power by varying crank angular velocity to increase the time spent in the powerful leg extension phase within the pedal cycle. Despite this sound theory of noncircular chainrings manipulating the instantaneous crank angular velocity to increase maximal cycling power, chainring eccentricity did not influence maximum cycling power and optimal pedaling rate. Plausible causes that negate the effects of the noncircular chainring include joint-specific redundant degrees of freedom (14, 24), low eccentricity, insufficient time for muscle excitation and relaxation (28), and crank orientation.

Joint-specific Redundant Degrees of Freedom

Two previous investigations reported improvements in maximal cycling performance with the use of noncircular chainrings (32, 34). O'Hara and colleagues (32) evaluated average power using a fatiguing 1km time trial protocol. In contrast, the only investigation to have evaluated the influence of noncircular chainrings on maximal cycling power utilized a theoretical model (34). This theoretical model predicted that an optimal chainring eccentricity of 1.29 would increase maximum cycling power by 2.9%. Although these investigators provided a detailed musculoskeletal model, the degree to which the simulated pedal angle influenced the kinematics of the ankle, knee, and hip joints remained unclear, as joint-specific kinematics were not reported. Interestingly, Martin and Brown (24) reported that cyclists exploited redundant degrees of freedom during the cycling action to perform ankle, knee, and hip extension for more than half the time for the pedal cycle. The multiple degrees of freedom in the leg, crank, and pedal

system may allow the manipulation of joint angular velocity with substantial independence from crank angular velocity and potentially negate the effects of the noncircular chainrings. Hence, it is plausible that cyclists may produce greater ankle joint excursion as a strategy to preserve/maintain hip and knee extension actions as the dominant power producing actions during maximal cycling. Within the scope of this present study, the degree to which a noncircular chainring influences joint-specific kinematics and joint-specific strategies for power production during maximal cycling remains speculative. Future work involving the evaluation of joint-specific kinematics and power will provide a more complete description of the influence of noncircular chainrings on maximum cycling power.

Chainring Eccentricity

To the best of my knowledge, this is the only study to have evaluated maximum cycling power experimentally and observed no differences in maximum cycling power between circular and noncircular chainrings. These results suggest that any potential to improve maximal cycling performance with the use of noncircular chainrings, if present at all, was not sufficient to measurably increase maximum cycling power. However, it is possible that the results were influenced by the magnitudes of chainring eccentricities utilized in this study. That is, the eccentricities (1.10 and 1.24) of the commercially available noncircular chainrings utilized in this study, may have been too low to elicit any measurable increase in maximum cycling power as compared to the predicted optimal eccentricity of 1.29 (34). Hence, a future direction may be to evaluate maximum cycling

power with the use of a noncircular chainring of eccentricity similar to or greater than 1.29.

Maximum Cycling Power and Optimal Pedaling Rate

Maximum cycling power and optimal pedaling rate were not significantly different between circular and noncircular chainring conditions. In addition, interpolated power produced at pedaling rates of 90 and 120 rpm did not differ between chainring conditions. In contrast, power produced at a pedaling rate of 150 rpm was reduced in the O (eccentricity 1.24) chainring condition compared to the circular condition. These results indicated a trend of decreasing power with increasing chainring eccentricity occurred at high pedaling rates (Figure 2.2B). Noncircular chainring manufacturers claim that a noncircular chainring shape slowed down the crank during the powerful extension phase maximizing the time spent producing power. In addition, a noncircular chainring shape can also minimize the time spent through the transition between extension and flexion, theoretically permitting a decrease in energy expenditure. While the benefit from minimizing the time spent in the transition phases is plausible, time spent in these regions may actually be beneficial to power production. During maximal cycling, muscle excitation occurs prior to shortening and the muscle remains excited for a larger portion of the shortening phase to increase work production (4, 12). Noncircular chainrings designed to minimize the time spent in relaxation may produce an unintended consequence of insufficient time for muscle excitation and relaxation. This could result in reduced excitation during muscle shortening (reduced force and power) and incomplete relaxation during lengthening (increased negative work) (4), especially at

high pedaling rates. Consequently, a reduced time for muscle excitation and relaxation within the transition phases may offset the intended gains of spending more time in the power producing phases with the use of a noncircular chainring. Direct measures of muscular activation levels (e.g., electromyography) during maximal cycling could provide more information regarding the possible changes induced by manipulations of pedaling rates and chainring eccentricity.

Placebo Effect

In this study, we minimized the possibility of a placebo effect by blinding the participants to each chainring condition. Although participants achieved a higher level of accuracy in perceiving the O compared to the C and R chainring conditions, maximal cycling performance between chainring conditions did not reflect a perceived treatment benefit. In contrast, O'Hara and colleagues (32) evaluated average power in a 1km time trial without blinding participants to chainring conditions. Because the placebo effect, ranging from magnitudes of 1% to 6%, has been implicated in improvements in sports performance (2, 3, 6, 21), it is plausible that the 6% significant increase in average power with Rotor Q-Rings over circular chainrings, could be a result of a placebo effect rather than a treatment/chainring effect.

Crank Orientation

An important part of our experimental design was that we maximized the effect of eccentricity within the portion of the pedal cycle that elicits the highest net cycling power (14, 24). The crank orientations utilized in this investigation were such that the smallest

radii (minor axis) were encountered at the beginning of the whole leg extension phase during maximal cycling (14). Because the whole leg extension phase occurs between the crank angles of 333°–165°, it is critical to ensure that the noncircular chainrings impose the largest portion of their eccentricities within this phase. Further, these crank orientations enabled the lowest crank angular velocities to occur within the whole leg extension phase (333°–165°). Thus, we oriented the noncircular chainrings to take maximum advantage of their shape to increase cycling power. Interestingly, the crank orientations recommended by the noncircular chainring manufacturers (e.g., Rotor) do not take full advantage of their shape and thus our results likely differ from previous investigations (32, 34) which utilized the recommended orientation.

Summary

In summary, maximum cycling power and optimal pedaling rate did not differ between circular and noncircular chainrings. These findings indicate that the use of noncircular chainrings did not enhance or compromise maximal cycling performance in these trained cyclists. We speculate that this negative result could be due to reduced time for muscle excitation and relaxation within the transition phases, thus offsetting the intended gains of spending more time in the power producing phases especially at high pedaling rates. Alternatively, the multiple degrees of freedom in the leg, crank, and pedal system may allow the manipulation of joint angular velocity in such a way as to negate the effects of the noncircular chainrings. A study incorporating the evaluation of joint-specific kinematics and/or electromyography could reveal the extent to which noncircular

chainrings influence joint-specific angular velocities and muscle coordination strategies during maximal cycling.

Table 2.1: Study 1 participant descriptive characteristics (n = 13).

	Mean±SD
Age (yr)	22±2
Mass (kg)	69±13
Height (m)	1.7±0.1

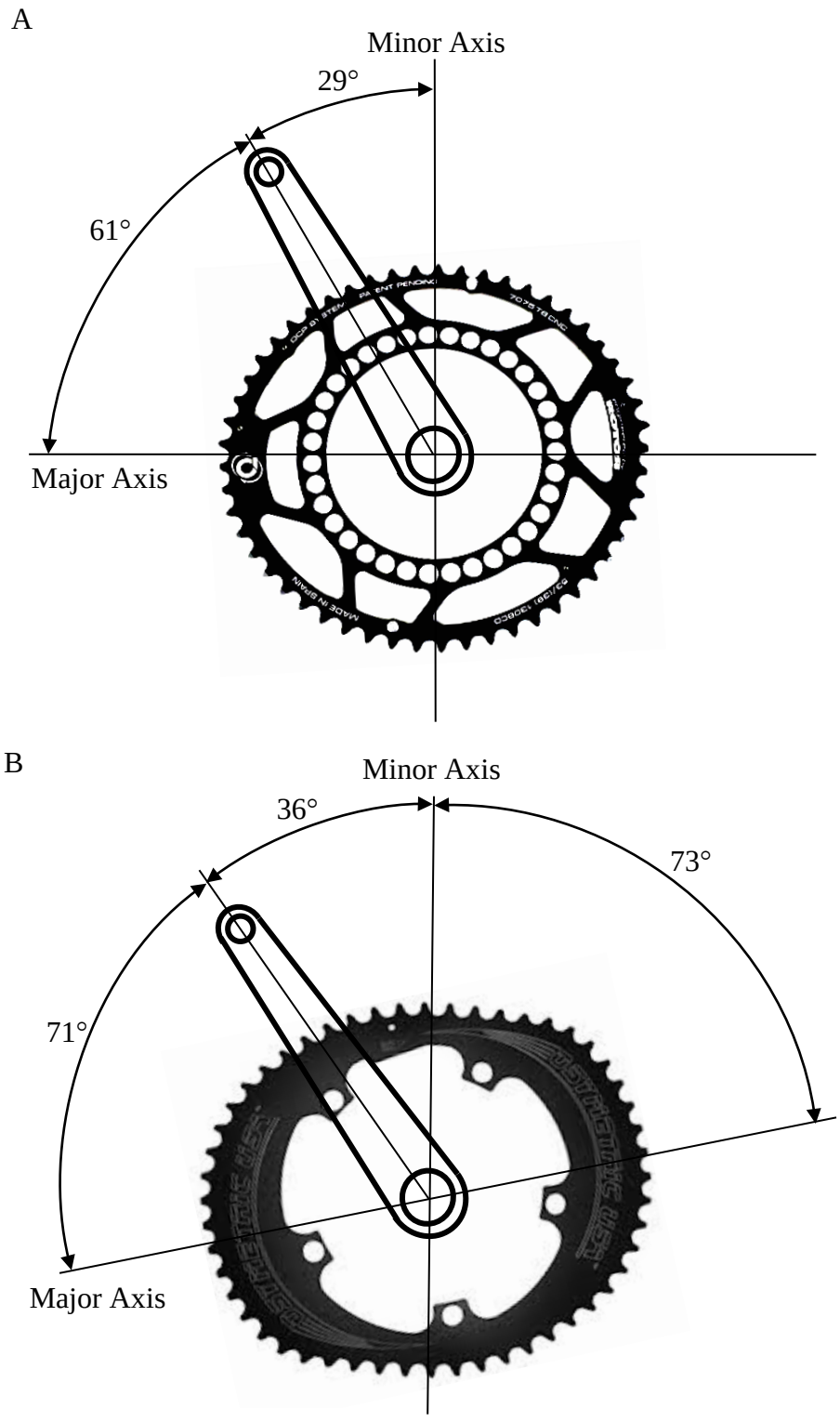

Figure 2.1: Geometries of the Rotor (R) and Osymetrics (O) chainrings. The shape of the R chainring is described as an ellipse where the major and minor axes are perpendicular. The R crank arm will be oriented at 61° forward of the major axis and 29° behind the minor axis (A). The shape of the O chainring is described as a skewed ellipse where the major and minor axes are not perpendicular, with the major axis oriented at 73° forward of the minor axis (B). The O crank arm will be oriented at 71° forward of the major axis and 36° behind the minor axis.

Table 2.2: Maximum cycling power and optimal pedaling rates produced during maximal cycling. Data presented as mean±SEM.

	Chainring Conditions		
	C	**R**	**O**
P_{max} (W)	1157±273	1148±259	1127±250
RPM_{opt} (rpm)	126±13	123±9	122±14

C, Circular; R, Rotor; O, Osymetric.
P_{max}, maximum cycling power.
RPM_{opt}, optimal pedaling rate that elicited maximum cycling power.

A

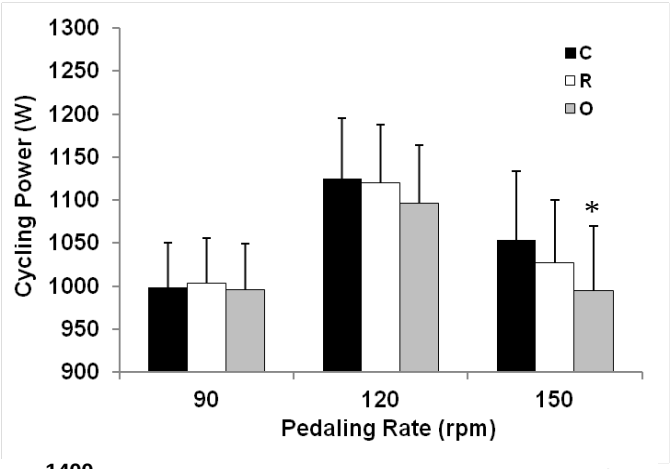

B

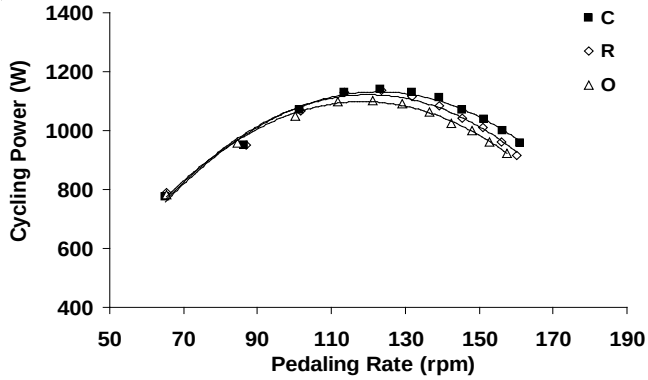

C

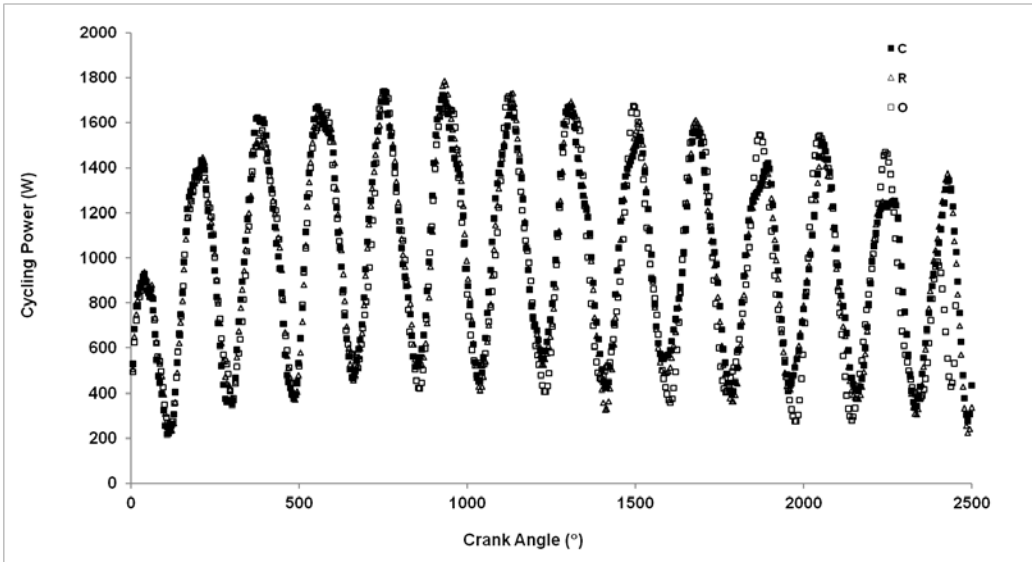

Figure 2.2: Cycling powers at pedaling rates of 90, 120, and 150 rpm interpolated from the power-pedaling rate relationships for each chainring condition (A). Complete power-pedaling rate relationships (B) and instantaneous power (C) for the C, R and O, chainring conditions (B). Values are presented as mean±SEM. SEM bars in panel B and C were removed for clarity. * $p < 0.05$ versus C chainring condition.

CHAPTER 3

EFFECTS OF NONCIRCULAR CHAINRINGS ON JOINT-SPECIFIC KINEMATICS AND POWER PRODUCTION DURING MAXIMAL CYCLING

Net cycling power is mainly produced during leg extension and flexion actions, whereas very little power is produced during the transition between extension and flexion (14). A strategy to maximize maximal cycling power within the pedal cycle is to increase the time spent in extension and flexion, while decreasing the time spent in the transition (14, 28). This optimization strategy allows a greater portion of the time spent in the high power producing phases within the pedal cycle. Circular chainrings result in a relatively constant angular velocity throughout the pedal cycle. Noncircular chainring profiles vary crank angular velocity and thus alter the time spent in each portion of the crank cycle (10, 20, 34, 35). For instance, a smaller chainring radius for some section of the cycle would increase crank angular velocity and decrease the time spent in that section. In contrast, a larger chainring radius for some section of the cycle would decrease angular velocity and increase the time spent in that section. Consequently, manufacturers of noncircular chainrings claim that increasing the time spent in the powerful extension and flexion actions while reducing the time spent in the transition phases will facilitate greater power production.

The only study to have evaluated the influence of noncircular chainrings on maximal cycling performance reported significant increases in maximum cycling power (34). These authors used a musculoskeletal modeling approach and reported that a noncircular chainring of average eccentricity of 1.29 could theoretically increase maximum cycling power by approximately 2.9% over a range of pedaling rates (60, 90, and 120 rpm). This result supports the notion to minimize the time spent in transition phases and maximize the time spent in the high power producing phases is plausible.

The degree to which instantaneous crank angular velocity will influence muscle and joint actions depends on the DOF in the leg, crank, pedal system. If the hip joint were fixed and the ankle joint center rotated about the pedal spindle, then the leg/crank/pedal system would have a single DOF and crank angular velocity would completely determine hip and knee joint angular velocities. However, angular movement of the ankle and linear movement of the hip joint center represent additional DOF in the system. These additional DOF allow the cyclist to manipulate joint angular velocities independent of crank angular velocity. In fact, Martin and Brown (24) reported that cyclists exploited redundant degrees of freedom (DOF) during maximal cycling to perform ankle, knee, and hip joint extension actions for more than half of the pedal cycle. Thus, cyclists instinctively increase the time spent in the extension action, and thereby increase cycling power. Consequently, the extent to which noncircular chainrings will provide additional benefit during voluntary maximal cycling remains unknown.

To my knowledge, no previous investigators have experimentally evaluated the influence of chainring eccentricity on cycling performance by analyzing joint-specific kinematics and power production. Therefore, the purpose of this investigation was to

evaluate the effects of noncircular chainrings on joint-specific kinematics and power production during maximal cycling. Based on the additional DOF that allow the cyclist to manipulate joint angular velocity with substantial independence from crank angular velocity, I hypothesized that the noncircular chainring's ability to influence cycling power through the manipulation of joint angular velocity, would be negated by the multiple DOF in the leg/crank/pedal system.

Methods

Participants

Ten trained cyclists licensed as category 3 or 4 by USA Cycling volunteered for this investigation (participant characteristics are presented in Table 3.1). None of the participants had previous experience in using noncircular chainrings. Experimental procedures used in this investigation were reviewed and approved by the University of Utah Institutional Review Board. The protocol and procedures were explained verbally, and all participants provided written informed consent prior to testing. Participants performed three familiarization sessions of maximal cycling trials on an isokinetic cycle ergometer (described below) the week before the experimental data collection. The cycle ergometer was configured such that participants were blinded to each chainring eccentricity. Because participants could sense differences in the pedaling action, they were asked to provide their perception of the chainring used for the cycling trials at the end of each testing session. The ergometer seat height was adjusted to match each participant's accustomed cycling position.

Experimental Protocol

Participants performed three familiarization sessions with each chainring eccentricity during the week prior to experimental data collection. During each of the three familiarization sessions, participants performed a 5 min warm-up (100–150 W, 90 rpm) of steady state normal cycling using one of the three randomly assigned chainring conditions. Participants then performed two seated maximal cycling trials of 3 s with 2 min resting recovery for each randomly assigned pedaling rates (60, 90, and 120 rpm). This protocol was repeated on each of the three experimental data collection days. Pedaling rates were matched between chainring conditions as the results from the first study demonstrated that the power-pedaling rate relationship, maximum power (P_{max}), and optimal pedaling rate (RPM_{opt}) were not altered by chainring eccentricity.

Chainring Conditions

The cycle ergometer was configured with chainring conditions of eccentricities (ratio of major-to-minor axis) 1.0, 1.13, and 1.24, using a conventional 53 tooth circular (C) chainring, a 53 tooth Rotor Q-Ring (R), and a 54 tooth Osymetrics (O) chainring, respectively. The shape of the R chainring is described as an ellipse where the major and minor axes are perpendicular (Figure 2.1A). The shape of the O chainring is described as a skewed ellipse where the major and minor axes are not perpendicular, with the major oriented at 61° forward of the minor axis (Figure 2.1B). Because the R and O chainrings have been designed to prolong the time spent in the leg extension phase, the crank arms for the R and O chainrings were oriented such that the smallest chainring radii are encountered (minor axes) at the beginning phase of whole leg extension during maximal

cycling. More precisely, the radius of the R and O chainrings progressively increased, reaching their maximum within the complete whole leg extension range of 333° to 165° typically observed with a C chainring (14). Consequently, the R crank arm was oriented at 61° forward of the major axis and 39° behind the minor axis (Figure 2.1A), and the O crank arm was oriented at 71° forward of the major axis and 36° behind the minor axis (Figure 2.1B).

The crank angular velocity profiles for the C, R, and O chainring conditions at the pedaling rates of 60, 90, and 120 rpm are presented in Figure 3.1. The crank arm orientations of the R and O chainrings (Figure 2.1) enabled these chainrings to impose approximately 80% of their eccentricities (ECC80) between the crank angles of 29° and 129°. In addition, work done within ECC80 accounted for 67% of the total work done within the whole pedal cycle. Consequently, the lowest crank angular velocities occurred during ECC80 within the whole leg extension phase in the R and O chainring conditions. The R and O chainring conditions produced sinusoidal crank angular velocity profiles compared to the C chainring condition. The R and O chainring conditions producing the lowest crank angular velocities at crank angles near 69° and the highest velocities near 159°, respectively. The lowest crank angular velocities in the R and O chainring conditions corresponded to the positions where the chainrings radii were near maximum (major axes). The highest crank angular velocities in the R and O chainring conditions corresponded to the positions where the chainring radii were near minimum (minor axes).

Isokinetic Ergometer

An isokinetic ergometer constructed using a Monark (Vansbro, Sweden) cycle ergometer frame and flywheel was used in this experiment. The flywheel was driven by a 3750-W direct-current motor (Baldor Electric Co. model CDP3605; Fort Smith, AR) via pulleys and a belt. The motor was controlled by a speed controller (Minarik model RG5500U; Glendale, CA) augmented with feedback (DLC600; Minarik) and a mechanical brake. The mechanical brake (standard Monark ergometer pendulum augmented with a 2-kg additional mass) forced the motor to function in driving mode rather than braking mode throughout the cycling trial. The right pedal of the isokinetic ergometer was equipped with two three-component piezoelectric force transducers (Kistler 9251; Kistler USA, Amherst, NY), and the right pedal and crank were equipped with digital position encoders (US Digital model S5S-1024; Vancouver, WA).

Kinematic and Kinetic Data

Two-dimensional kinematic and kinetic data were obtained using the methods originally described by Martin and colleagues (27). Briefly, pedal forces, pedal and crank positions, and the position of an instrumented spatial linkage system (ISL) were recorded at 240 Hz using Bioware software 3.0 (Kistler USA). Normal and tangential pedal forces, pedal position, crank position, and ISL position data were filtered using a fourth-order zero-lag low-pass Butterworth filter with a cutoff frequency of 8 Hz. Pedal power was calculated as the dot product of pedal force and linear pedal velocity. Positions of the right greater trochanter and iliac crest were determined by collecting a static trial of each participant attached to the ISL, and the relative position was assumed

to remain constant (31). During the cycling protocols, recorded iliac crest, pedal, and crank position coordinates allowed sagittal plane limb segment positions to be determined using law of cosines. Linear and angular velocities and accelerations of the limb segments were determined by finite differentiation of position data. Segmental masses, moments of inertia, and location of centers of mass were estimated using the regression equations (11). Sagittal plane joint reaction forces and net joint moments at the ankle, knee, and hip were determined by using inverse dynamics techniques (13). Ankle, knee, and hip joint–specific powers were calculated as the product of net joint moments and joint angular velocities. Power transferred across the hip joint was calculated as the dot product of the hip joint reaction force and linear velocity. Joint-specific powers were analyzed for 3 s and were averaged over all of the complete pedal cycles within the 3-s measurement interval. Additionally, joint-specific powers were averaged over the extension and flexion phases, which will be defined by joint angular velocity directions (24). Because most power was produced during the extension phase, power values averaged over the extension phase can be larger than those averaged over complete pedal cycles, and consequently, the sum of these relative joint-specific power values can exceed 100%. Duty cycle values for the whole leg were based on the magnitude of the position vector from the hip joint to the pedal spindle, with extension defined as an increasing magnitude and flexion as a decreasing magnitude. Ankle, knee, and hip joint duty cycle values were calculated as the ratio of the time for extension to the time for flexion. Note that joint duty cycle values can sometimes be < 1.0, whereas whole-leg duty cycle values are close to or > 1.0 because of linear movement of the hip joint center.

Data Analysis

Separate two-way (pedaling rate × eccentricity) repeated measures analysis of variance (ANOVA) were performed to assess differences in crank angular velocity, joint-specific angular velocities produced during ankle, knee, and hip extension, within the whole leg extension phase and ECC80 for the C, R, and O chainring conditions. Separate two-way (pedaling rate × eccentricity) repeated measures ANOVA were also performed for power produced at the pedal, and during ankle, knee, and hip extension within the whole leg extension phase and ECC80 for the C, R, and O chainring conditions. A one-way repeated measures analysis of variance (ANOVA) was also used to evaluate chainring perception across the different chainring conditions.

If these individual ANOVA indicated a significant main effect or significant interactions, pair-wise comparisons using Fisher's least significant difference post hoc analyses were used to identify where those differences occurred. All data are presented as mean±standard error of the mean (SEM) and alpha was set to 0.05.

Results

Whole Leg Extension Phase

The repeated measures ANOVA revealed a significant effect of pedaling rate on crank angular velocity ($p < 0.01$; Figure 3.1; Table 3.2) and joint-specific angular velocities ($p < 0.01$; Figure 3.2; Table 3.2) produced during ankle, knee, and hip extension. Subsequent post hoc analyses indicated crank angular velocity and joint-specific angular velocities produced during ankle, knee, and hip extension increased with increasing pedaling rates of 60, 90, and 120 rpm (all $p < 0.01$; Table 3.2). Crank angular

velocity and joint-specific angular velocities produced during ankle, knee, and hip extension did not differ between the C, R, and O chainring conditions and the pedaling rate × eccentricity interactions were not significant (all $p > 0.05$).

Repeated measures ANOVA revealed a significant effect of pedaling rate on pedal power ($p < 0.05$; Figure 3.3; Table 3.3), and power produced during knee and hip extension ($p < 0.05$; Figure 3.4; Table 3.3) for the C, R, and O chainring conditions. Power produced during ankle extension did not differ between pedaling rates ($p = 0.10$). In addition, pedaling rate × eccentricity interactions were not significant (all $p > 0.05$). Subsequent post hoc analyses indicated pedal power, and power produced during knee and hip extension increased with increasing pedaling rates of 60, 90, and 120 rpm (all $p < 0.05$; Table 3.3).

ECC80 (Crank angle of 27°–129°)

The repeated measures ANOVA revealed a significant effect of pedaling rate ($p < 0.01$; Figure 3.1; Table 3.2) on crank angular velocity and joint-specific angular velocities produced during ankle, knee, and hip extension within ECC80. Subsequent post hoc analyses indicated that crank angular velocity and joint-specific angular velocities produced during ankle, knee, and hip extension within ECC80 increased with increasing pedaling rates of 60, 90, and 120 rpm (all $p < 0.01$; Table 3.2). The repeated measure ANOVA also revealed a significant effect of eccentricity on crank angular velocity ($p < 0.01$; Figure 3.1; Table 3.2), and pedaling rate × eccentricity interaction for ankle angular velocity within ECC80 ($p < 0.05$; Figure 3.2; Table 3.2). Pedaling rate × eccentricity interactions for knee and hip angular velocities were not significant (all $p >$

0.05; Table 3.2). Subsequent post hoc analyses indicated that crank angular velocities of the R chainring condition were 1.9±0.6%, 2.2±0.3%, and 2.2±0.4% lower than the C chainring condition at pedaling rates of 60, 90, and 120 rpm, respectively (both $p < 0.05$; Figure 3.1; Table 3.2). The crank angular velocities of the O chainring condition were 4.7±0.5%, 4.6±0.2%, and 4.8±0.2% lower than the C chainring condition at pedaling rates of 60, 90, and 120 rpm, respectively (all $p < 0.05$; Figure 3.1; Table 3.2). In addition, the crank angular velocities of the O chainring condition were 2.8±0.5%, 2.5±0.3%, and 2.6±0.5% lower than the R chainring condition at pedaling rates of 60, 90, and 120 rpm, respectively (all $p < 0.05$; Figure 3.1; Table 3.2). Subsequent post hoc analyses also indicated that the angular velocity produced during ankle extension within ECC80 with the O chainring was 13±12% lower than C and 22±5% lower than R at 90 rpm (all $p < 0.05$; Figure 3.2; Table 3.2). Ankle extension within ECC80 with the O chainring was 37±13% lower than C at 120 rpm ($p < 0.05$; Figure 3.2; Table 3.2).

Repeated measures ANOVA revealed a significant effect of pedaling rate on pedal power ($p < 0.05$; Figure 3.3; Table 3.3), and power produced during ankle, knee, and hip extension ($p < 0.05$; Figure 3.4; Table 3.3) within ECC80. Pedal power and power produced during ankle, knee, and hip extension within ECC80 did not differ between chainring conditions (all $p > 0.05$; Table 3.3). In addition, pedaling rate × eccentricity interactions were not significant (all $p > 0.05$; Table 3.3). Subsequent post hoc analyses indicated power produced at the pedal, and during ankle, knee, and hip extension within ECC80 increased with increasing pedaling rates of 60, 90, and 120 rpm (all $p < 0.05$; Table 3.3).

Chainring Perception

Repeated measures ANOVA revealed no significant differences in chainring perception between the C, R, and O chainring conditions ($p = 0.63$). Participants achieved 80±13%, 70±15%, and 60±16% accuracy in chainring perception for the C, R, and O chainring conditions, respectively.

Discussion

Noncircular chainrings alter crank angular velocity within each cycle and can be oriented to increase the time required for the pedal to move through a specific angular displacement. Prolonging the time spent in the powerful leg extension and flexion actions and reducing the time spent in the transition phases might be expected to increase average power for a complete cycle. It is important to note, however, that power delivered to cycling cranks is produced mainly by muscular hip extension, knee extension, and knee flexion (14, 24). Consequently, a noncircular chainring will only be beneficial if it is successful at altering those joint actions. Despite a noncircular chainring's ability to manipulate crank angular velocity to theoretically allow muscles to generate power longer, the main finding from this study was that noncircular chainrings did not improve maximum cycling power and joint-specific power during maximal cycling. In addition, knee and hip angular velocities remained unaffected with only ankle angular velocity influenced by chainring eccentricity. Collectively, these results suggest that multiple DOF in the leg, crank, and pedal system allowed the manipulation of joint angular velocity at the ankle in such a way as to negate the effects of the noncircular chainrings during maximal cycling. That is, the effects of the chainring on crank angular

velocity were eliminated by these cyclists' ankling action and thus did not alter the major power producing actions of the hip and knee.

Rankin and Neptune (34) were the only investigators to evaluate the influence of noncircular chainrings on maximum cycling power. They utilized a musculoskeletal model rather than human participants. Their model predicted that a chainring with an eccentricity of 1.29 would improve cycling power by approximately 3%. Chainrings with such large eccentricity are not readily available and we were unable to obtain one for this investigation. Thus, our results do not contradict those of Rankin and Neptune (34) because we did not use their model-predicted chainring shape. Even so, it would be very interesting to know if their model adopted different ankle velocities for the various chainring conditions and if perturbations by the chainring actually influenced hip and knee actions.

Although they did not specifically study maximum power, O'Hara and colleagues (32) did investigate power during a maximal fatiguing effort of approximately 84 s. They reported a 6% increase in average power during a 1km time trial with Rotor Q-Rings over circular chainrings. Since we did not measure power during a fatiguing effort, we cannot comment on how our results compare with theirs. However, it is important to note that they did not report pedaling rates for their conditions. Instead, they stated that participants self-selected gears for each condition. Thus, it is possible that those participants selected gears that gave them a less fatiguing pedaling rate for the noncircular chainring condition. Further, because their participants were not blinded to the chainring conditions, it is also possible that their results represent a placebo or belief effect, which can influence performance by up to 6% (1, 2, 6, 21).

Chainring Perception

The cycle ergometer utilized in this study was configured such that participants were blinded to each chainring condition in order to control for a favorable outcome arising purely from the perception of receiving a benefit from a noncircular chainring. Participants achieved similar levels of accuracy in perceiving all chainring conditions. Firstly, this result may suggest that the chainring blinding procedure was effective in controlling for a placebo effect. Secondly, it also suggests that participants were unable to differentiate between the chainrings despite being able to anecdotally detect the chainring with the largest eccentricity (O chainring condition) at the first 2 min of their warmup trial. Several participants made anecdotal claims that they were able to perceive a noncircular chainring as it gave them the sensation that they were "galloping." However, these participants would claim that they have "gotten used to" cycling with a noncircular chainring when the "galloping" sensation ceased/dissipated postcycling trials and failed to identify the chainring at the 5 min time point. Taken together, the lack of differences in chainring perception and the anecdotal experience of "getting used to" cycling with a noncircular chainring, may further emphasize a negation effect through the redundant degree of freedom at the ankle. It also implies that alterations to the drive train with a noncircular chainring may or may not be immediately evident with competitive cyclists accustomed to pedaling with circular chainrings. Because the transition from a circular to noncircular chainring introduced a change in pedaling dynamics, a future direction would be to evaluate the time-course of alterations in joint-specific kinematics by tracking these alterations (if any) over the familiarization/learning period.

Summary

This is the first investigation to compare joint-specific kinematics and power production with circular and noncircular chainrings during maximal cycling across a range of pedaling rates. Despite a noncircular chainring's ability to manipulate crank angular velocity, its eccentricity only influenced ankle angular velocity, while knee and hip angular velocities remained unaffected during the powerful extension phase. Thus, the trained cyclists in this study were able to defend the angular velocities produced during knee and hip extension by exploiting the additional DOF at the ankle to protect against perturbations at the crank. Nonetheless, the efficacy of the noncircular chainrings on influencing maximal cycling performance cannot be entirely refuted since the eccentricities (1.10 and 1.24) utilized in this investigation were lower than the optimal eccentricity of 1.29 predicted by Rankin and Neptune (34). Taken together, the results from this present study and those by previous investigators (14, 24, 28), serve to emphasize the multijoint complexity in the cycling action, and also suggest that an eccentricity beyond those commercially available, may be effective in improving maximal cycling performance.

Table 3.1: Study 2 participant descriptive characteristics (n = 10).

	Mean±SD
Age (yr)	34±7
Mass (kg)	72±9
Height (m)	1.8±0.1

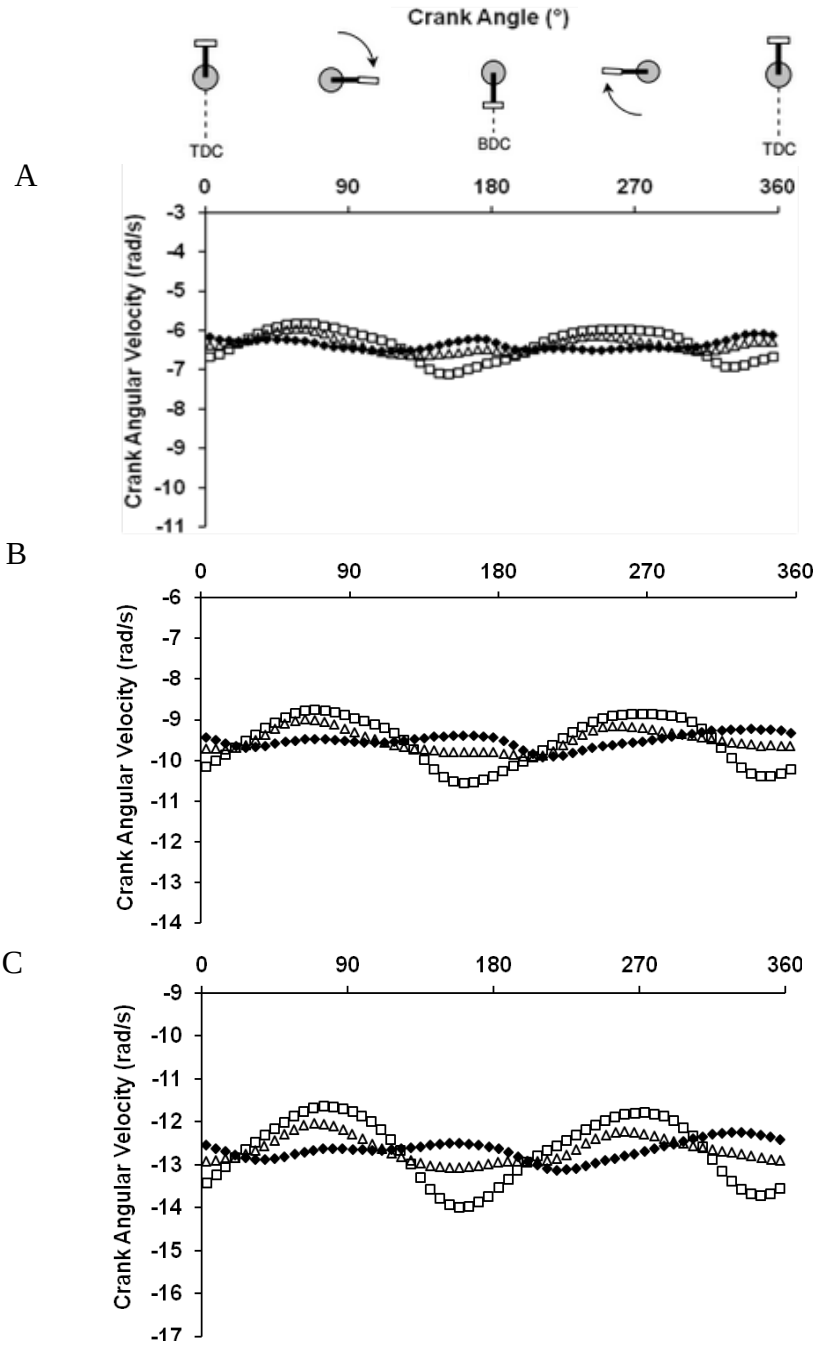

Figure 3.1: Crank angular velocity profiles of the C (◆), R (Δ), and O (□) chainring conditions at the pedaling rates of 60 rpm (A), 90 rpm (B), and 120 rpm (C). Crank angles of 0° and 360° represent the top dead center position, and 180° represents the bottom dead center position. The R and O chainring conditions produced relatively sinusoidal crank angular velocity profiles with 5% and 8% variation, respectively, compared to the C chainring condition. The R and O chainring conditions both produced the lowest crank angular velocities at crank angles near 69° and the highest velocities near 159°. The lowest crank angular velocities during the whole leg extension phase in the R and O chainring conditions corresponded to crank angles between 27° and 129°.

Table 3.2: Joint-specific angular velocity produced during whole leg extension phase and ECC80 (crank angle of 27°–129°) at pedaling rates of 60, 90, and 120 rpm. Data presented as mean±SEM.

Angular Velocity (rad/s)	Pedaling Rate								
	60 rpm			90 rpm			120 rpm		
	C	R	O	C	R	O	C	R	O
Whole Leg Extension Phase									
Crank[a]	–6.36±0.01	–6.35±0.01	–6.36±0.01	–9.51±0.01	–9.49±0.02	–9.50±0.01	–12.65±0.02	–12.62±0.02	–12.65±0.02
Ankle Extension[a]	–1.38±0.12	–1.42±0.10	–1.46±0.13	–1.95±0.13	–2.01±0.15	–1.95±0.15	–2.05±0.19	–2.31±0.20	–2.18±0.18
Knee Extension[a]	2.65±0.14	2.66±0.13	2.71±0.12	3.76±0.07	3.94±0.16	3.96±0.13	4.96±0.12	4.98±0.20	5.05±0.17
Hip Extension[a]	–1.56±0.09	–1.60±0.09	–1.56±0.07	–2.25±0.09	–2.30±0.14	–2.39±0.10	–3.28±0.12	–3.27±0.13	–3.29±0.12
ECC80									
Crank[a,b]	–6.38±0.03	–6.26±0.03[*]	–6.08±0.02[*,#]	–9.54±0.02	–9.33±0.03[*]	–9.10±0.02[*,#]	–12.71±0.03	–12.43±0.04[*]	–12.10±0.03[*,#]
Ankle Extension[a,b]	–1.25±0.19	–1.25±0.17	–1.27±0.16	–1.49±0.24	–1.62±0.24	–1.28±0.23[*,#]	–0.90±0.28	–0.83±0.28	–0.59±0.25[*]
Knee Extension[a]	3.29±0.20	3.26±0.17	3.16±0.15	4.82±0.16	4.88±0.22	4.77±0.18	6.45±0.19	6.42±0.23	6.32±0.24
Hip Extension[a]	–1.91±0.15	–1.94±0.13	–1.85±0.11	–2.80±0.15	–2.81±0.18	–2.76±0.16	–3.92±0.14	–3.97±0.17	–3.92±0.16

[*] Significantly lower than C condition ($p < 0.05$).

[#] Significantly lower than R condition ($p < 0.05$).

[a] Main effect of pedaling rate ($p < 0.01$).

[b] Pedaling rate × eccentricity ($p < 0.05$).

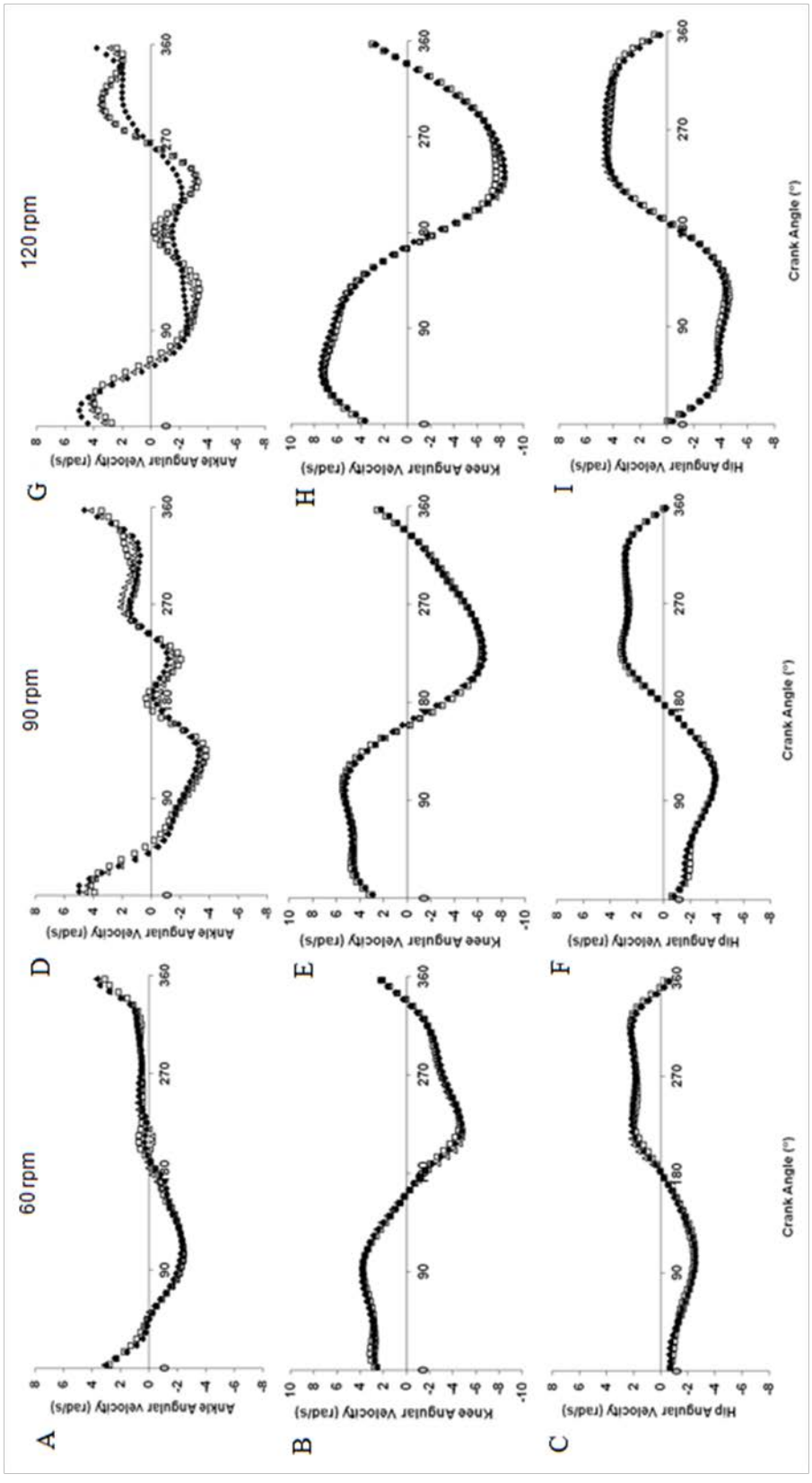

Figure 3.2: Joint-specific mean angular velocities versus crank angle for the C (◆), R (Δ), and O (□) chainring conditions during maximal cycling at pedaling rates of 60 rpm (left column), 90 rpm (center column), and 120 rpm (right column). Crank angles of 0° and 360° represent the top dead center (TDC) position, and 180° represents the bottom dead center (BDC) position.

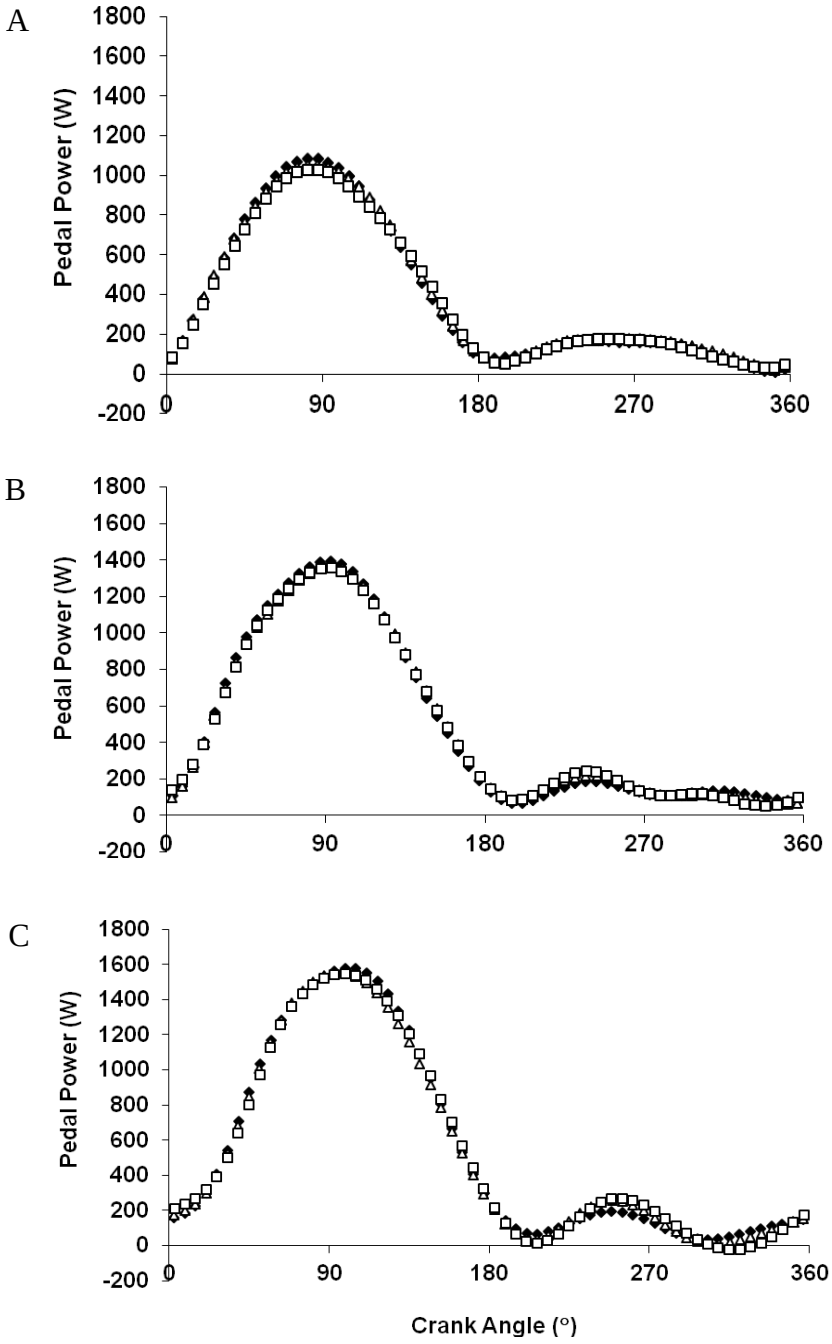

Figure 3.3: Power versus crank angle for C (◆), R (Δ), and O (□) chainring conditions. Mean power produced at the pedal during maximal cycling at 60 rpm (A), 90 rpm (B), and 120 rpm (C). Crank angles of 0° and 360° represent the top dead center position, and 180° represents the bottom dead center position. Note that power was measured at the right pedal, thus pedal and joint-specific powers represent the power produced by one leg.

Table 3.3: Power produced at the pedal, ankle, knee, and hip during whole leg extension phase and ECC80 (crank angle of 27°–129°) at pedaling rates of 60, 90, and 120 rpm. Data presented as mean±SEM.

Cycling Power (W)	Pedaling Rate								
	60 rpm			90 rpm			120 rpm		
	C	R	O	C	R	O	C	R	O
Whole Leg Extension Phase									
Pedal[a]	385±30	392±29	386±29	487±38	491±37	496±38	544±42	540±43	547±44
Ankle	58±8	59±8	59±7	68±8	70±8	66±9	69±8	67±9	67±9
Knee[a]	125±11	119±11	117±12	180±17	173±16	186±19	222±20	221±22	223±28
Hip[a]	168±14	181±15	180±14	196±16	207±14	201±14	216±19	219±21	225±24
ECC80									
Pedal[a]	891±63	883±63	848±58	1142±87	1116±86	1108±83	1243±93	1219±93	1209±89
Ankle[a]	164±25	168±23	162±23	169±26	184±24	164±25	104±22	117±22	110±20
Knee[a]	153±26	142±25	117±22	279±38	220±33	230±29	335±37	301±37	281±36
Hip[a]	378±38	394±36	392±32	431±38	471±42	461±39	487±43	511±48	520±45

[a] Main effect of pedaling rate ($p < 0.05$).

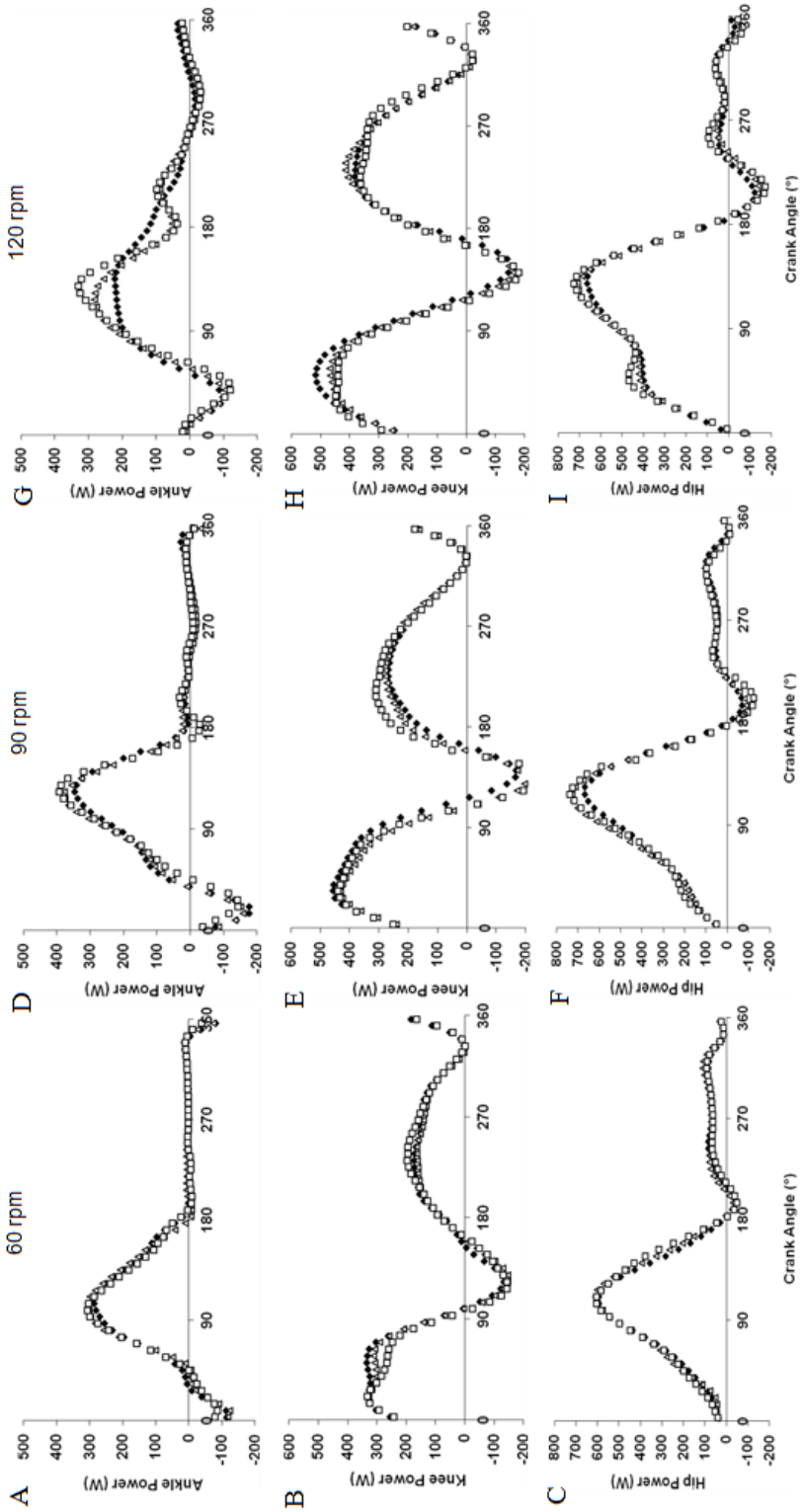

Figure 3.4: Joint-specific power versus crank angle for C (◆), R (Δ), and O (□) chainring conditions during maximal cycling at pedaling rates of 60 rpm (left column), 90 rpm (center column), and 120 rpm (right column). Crank angles of 0° and 360° represent the top dead center position, and 180° represents the bottom dead center position. Note that power was measured at the right pedal, thus pedal and joint-specific powers represent the power produced by one leg.

CHAPTER 4

EFFECTS OF NONCIRCULAR CHAINRINGS ON PHYSIOLOGICAL RESPONSES DURING SUBMAXIMAL CYCLING

Power output is the main determinant of metabolic cost during cycling, accounting for 95% of the variability across a wide range of conditions (30). Pedal speed (or pedaling rate if only a single crank length is used) has been shown to account for the majority of the remaining variability in metabolic cost and the combination of power and speed accounted for 98% of the variation in metabolic cost (30). Noncircular chainrings can alter instantaneous crank angular velocity, and thereby pedal speed. Reducing pedal speed during the portion of the cycle in which most power is produced, could reduce metabolic cost and increase metabolic efficiency. That is, most cycling power is produced within crank angles of 339°–161° during submaximal cycling (14). If a noncircular chainring were used in such a way as to reduce speed within that region, metabolic cost might be reduced.

Previous investigators who have evaluated the effect of noncircular chainrings on physiological responses during submaximal cycling have reported mixed results. Several investigators detected no physiological effects between circular and noncircular chainrings (7, 18, 20, 33, 35). One group reported a 22% reduction in blood lactate

concentration (15), when cyclists were allowed to self-select pedaling rates. Another group reported a 3% reduction in metabolic cost with concomitant increases in average cycling power (32) during a maximal 1km time trial. Thus, the efficacy of chainring shape/eccentricity on submaximal cycling performance remains equivocal.

A plausible explanation for the mixed findings of chainring shape/eccentricity on submaximal cycling performance could be the lack in the control of pedaling rate. For any specific pedaling rate, a noncircular chainring has slower pedal speed during the power producing phase compared to a circular chainring. Therefore, at the same pedaling rate a lower metabolic cost might be expected. It is also plausible that the metabolic cost would be equal when pedal speed within the power producing phase is matched. Thus, in previous investigations that evaluated submaximal cycling performance by varying the chainring shape/eccentricity alone, the metabolic cost associated with the use of a noncircular chainring cannot be differentiated from that associated with pedaling rate and/or pedal speed.

My primary purpose for conducting this investigation was to decouple the pedal speed from chainring shape/eccentricity by determining the separate contributions of pedal speed and chainring shape/eccentricity to the metabolic cost of producing submaximal cycling power. I hypothesized that a lower pedal speed, rather than larger eccentricity per se, would result in lower metabolic cost during submaximal cycling. A secondary purpose was to evaluate the effects of noncircular chainrings on joint-specific kinematics during submaximal cycling. Based on the additional DOF that allow the cyclist to manipulate joint angular velocity with substantial independence from crank angular velocity, I hypothesized that the noncircular chainring's ability to manipulate

joint angular velocity would be negated by the multiple DOF in the leg/crank/pedal system.

Methods

Participants

Eight trained cyclists (7 males and 1 female) licensed as category 3 or 4 by USA Cycling volunteered to participate in this investigation (participant characteristics are presented in Table 4.1). None of the participants had previous experience in using noncircular chainrings. Experimental procedures used in this investigation were reviewed and approved by the University of Utah Institutional Review Board. The protocol and procedures were explained verbally, and all participants provided written informed consent prior to testing. The cycle ergometer was configured such that participants were blinded to each chainring eccentricity. Because participants could sense differences in the pedaling action, they were asked to provide their perception of the chainring used for the cycling trials at the end of each testing session. The ergometer seat height was adjusted to match each participant's accustomed cycling position.

Experimental Protocol

Participants reported to the laboratory on five separate occasions. During the first visit, peak oxygen consumption ($\dot{V}O_{2peak}$) and lactate threshold (LT) were determined. After a 5-min warm-up at 100 W, the $\dot{V}O_{2peak}$ test commenced with the participants pedaling at 90 rpm for 5 min at 100 W on a Velotron Elite (RacerMate Inc., Seattle, Washington, USA) computer controlled, electromagnetically braked cycle ergometer.

The workrate was then increased 50 W every 5 min until volitional fatigue (38). $\dot{V}O_2$ and respiratory exchange ratio (RER) were calculated at 15 s intervals, and $\dot{V}O_{2peak}$ was calculated as the average of the highest two consecutive $\dot{V}O_2$ measurements. Blood was drawn during the 5th min of each stage and lactate concentrations were measured using Lactate Pro lactate analyzer (ARKRAY Lactate Pro LT-1710, Kyoto, Japan). LT was defined as the intensity at which blood lactate concentration increased to 1 mmol above baseline (8).

During the second laboratory visit, participants performed familiarization sessions with the C, O, and R chainrings. Participants cycled at a power output intended to elicit 60% of LT with each chainring. During each 25-min familiarization session, participants cycled for 5 min at pedaling rates of 80 rpm on the C, R, and O chainrings (C80, R80, and O80, respectively).

Experimental data were recorded during the remaining three laboratory visits. On each experimental visit to the laboratory anthropometric measurements were recorded. Specifically, body mass, height, thigh length (*greater trochanter* to *lateral femoral condyle*), leg length *(lateral femoral condyle* to *lateral malleolus*), foot length (heel to toe), and kinematic foot length (*lateral malleolus* to pedal spindle) were measured. On each experimental visit, participants performed the data collection protocol with one of three randomized chainring conditions. For each noncircular chainring condition, participants performed 5 min of steady state cycling at randomized workrates of 30, 60, and 90% of their LT power. After each noncircular chainring condition, participants would rest for 5 min before repeating the protocol with a circular chainring matched for

pedal speed. Throughout the experimental protocol, $\dot{V}O_2$, RER, and heart rate were recorded every 15 w and averaged over min 4–5 of each condtion.

Chainring Conditions

The cycle ergometer was configured with chainring conditions of eccentricities (ratio of major-to-minor axis) 1.0, 1.13, and 1.24, using a conventional 53 tooth circular (C) chainring, a 53 tooth Rotor Q-Ring (R), and a 54 tooth Osymetrics (O) chainring, respectively. The shape of the R chainring is described as an ellipse where the major and minor axes are perpendicular (Figure 2.1A). The shape of the O chainring is described as a skewed ellipse where the major and minor axes are not perpendicular, with the major oriented at 61° forward of the minor axis (Figure 2.1B). The R and O chainrings were oriented such that the smallest chainring radii are encountered (minor axes) at the beginning phase of whole leg extension during maximal cycling. More precisely, the radius of the R and O chainrings progressively increased, reaching their maximum within the complete whole leg extension range of 333° to 165° typically observed with a C chainring (14). Consequently, the R crank arm was oriented at 61° forward of the major axis and 29° behind the minor axis (Figure 2.1A), and the O crank arm was oriented at 71° forward of the major axis and 36° behind the minor axis (Figure 2.1B). This configuration allowed for reduced crank angular velocity during the leg extension phase where most power is produced.

The crank angular velocity profiles for the C, O, and R chainring conditions at the workrate of 90% LT power (representative of 30% and 60% LT power) are presented in Figure 4.1. The crank orientations of the R and O chainrings (Figure 2.1) enabled these

chainrings to impose approximately 80% of their eccentricities (ECC80) between the crank angles of 27° and 129°. In addition, work done within ECC80 accounted for 76% of the total work done within the whole pedal cycle. Consequently, the reduced crank angular velocities occurred during ECC80 within the whole leg extension phase in the R and O chainring conditions. The R and O chainring conditions produced crank angular velocity profiles that were generally sinusoidal, whereas the C chainring condition was nearly constant. The R and O chainring conditions produced the lowest crank angular velocities at crank angles near 69° and the highest velocities near 159°, respectively. The lowest crank angular velocities in the R and O chainring conditions corresponded to the positions where the chainrings radii were near maximum (major axes). The highest crank angular velocities in the R and O chainring conditions corresponded to the positions where the chainring radii were near minimum (minor axes).

Pedaling rates for C78 and C75 conditions were calculated by matching pedal speed of the C chaining condition to the average pedal speeds occurring within ECC80 of R80 and O80 conditions, respectively (Figure 4.1). Pedal speeds at C75 and C78 conditions corresponded to pedal speeds of approximately 0.85 m/s and 0.88 m/s for the O80 rpm and R80 conditions, respectively.

Metabolic Measures, Gross Efficiency, Delta Efficiency, and Cost of Unloaded Cycling

Gas exchange data were measured using open circuit spirometry (True Max 2400, Parvo Medics, Sandy, UT, USA). The metabolic system was calibrated by using room air and a calibration gas concentration (16.00% O_2, 4.00% CO_2, balanced N_2). Expired

air was analyzed via the metabolic cart and RER, HR, $\dot{V}CO_2$, and $\dot{V}O_2$ were all determined by 30-second averaged values obtained through analysis. Mechanical power was controlled by a Velotron Elite (RacerMate Inc., Seattle, Washington, USA) computer controlled, electromagnetically braked flywheel, which has been shown to be accurate and reliable (30).

Metabolic cost was calculated by the regression equation of Zuntz (41) based on the thermal equivalent of O_2 for nonprotein respiratory equivalent: metabolic cost (kcal/h) = $\dot{V}O_2 \times (1.2341 \times RER + 3.8124)$. Gross efficiency (GE) was calculated as the ratio of work generated to the metabolic cost.

Kinematic and Kinetic Data

Two-dimensional kinematic and kinetic data were obtained using the methods originally described by Martin and colleagues (24, 27). Briefly, pedal forces, pedal and crank positions, and the position of an instrumented spatial linkage system (ISL) were recorded at 240 Hz using Bioware software 3.0 (Kistler USA). Normal and tangential pedal forces, pedal position, crank position, and ISL position data were filtered using a fourth-order zero-lag low-pass Butterworth filter with a cutoff frequency of 8 Hz. Pedal power was calculated as the dot product of pedal force and linear pedal velocity. Positions of the right greater trochanter and iliac crest were determined by collecting a static trial of each participant attached to the ISL, and the relative position was assumed to remain constant (31). During the cycling protocols, recorded iliac crest and pedal and crank position coordinates allowed sagittal plane limb segment positions to be determined using law of cosines. Linear and angular velocities and accelerations of the

limb segments were determined by finite differentiation of position data. Segmental masses, moments of inertia, and location of centers of mass were estimated using the regression equations (11). Sagittal plane joint reaction forces and net joint moments at the ankle, knee, and hip were determined by using inverse dynamics techniques (13). Ankle, knee, and hip joint–specific powers were calculated as the product of net joint moments and joint angular velocities. Power transferred across the hip joint was calculated as the dot product of the hip joint reaction force and linear velocity. Joint-specific powers were analyzed for 3 s and were averaged over all of the complete pedal cycles within the 3-s measurement interval. Additionally, joint-specific powers were averaged over the extension and flexion phases, which were defined by joint angular velocity directions (24). Because most power was produced during the extension phase, power values averaged over the extension phase can be larger than those averaged over complete pedal cycles, and consequently, the sum of these relative joint-specific power values can exceed 100%.

Data Analysis

A two-way (pedal speed × workrate) repeated measures ANOVA were performed to assess differences in physiological variables ($\dot{V}O_2$, RER, Metabolic Cost, GE, HR, $RPE_{overall}$, RPE_{legs}) and joint-specific kinematics for the C80, R80, O80, C75, and C78 conditions. A two-way (pedal speed × workrate) repeated measures ANOVA was also performed to assess differences in joint-specific kinematics (crank and joint-specific angular velocity) produced during whole leg extension phase and ECC80 for the C80, R80, O80, C75, and C78 conditions. A one-way repeated measures analysis of variance

(ANOVA) was also used to evaluate chainring perception across the different chainring conditions.

If these individual ANOVAs indicated a significant main effect or significant interactions, pair-wise comparisons using Fisher's least significant difference post hoc analyses were used to identify where those differences occurred. All data are presented as mean±standard error of the mean (SEM) and alpha was set to 0.05.

Results

Metabolic Measures and Gross Efficiency

Mean values of physiological variables ($\dot{V}O_2$, RER, Metabolic Cost, GE, HR, $RPE_{overall}$, RPE_{legs}) for steady-state submaximal cycling at workrates of 30%, 60%, and 90% LT power are presented in Table 4.2. Repeated measures ANOVA revealed a significant effect of workrate (all $p < 0.01$), with no significant effects of pedal speed and no significant pedal speed × workrate interaction (all $p > 0.05$; Table 4.2; Figure 4.2), on physiological variables. Subsequent post hoc analyses indicated physiological variables increased with increasing workrates of 30%, 60%, and 90% LT power (all $p < 0.01$).

Joint-specific Kinematics for Whole Leg Extension Phase

The repeated measures ANOVA indicated no significant effect of workrate ($p > 0.05$; Table 4.3) and pedal ($p > 0.05$), and no significant pedal speed × workrate interaction ($p > 0.05$), on crank angular velocity, and angular velocity produced during ankle extension for the C80, R80, and O80, during the whole leg extension phase. Repeated measures ANOVA revealed a significant effect of workrate (all $p < 0.05$) on

angular velocities produced during knee and hip extension. Subsequent post hoc analyses indicated angular velocities produced during knee and hip extension increased with increasing workrates of 30%, 60%, and 90% LT power (all $p < 0.05$; Table 4.3).

The repeated measures ANOVA revealed significant effect of pedal speed ($p < 0.01$; Table 4.3), with no significant effect of workrate ($p > 0.05$) and no significant pedal speed × workrate interaction, on crank angular velocity, and angular velocity produced during ankle extension for the C80, R80, and C78, during the whole leg extension phase.

Subsequent post hoc analyses indicated crank angular velocity at the C78 condition was 3.4±0.5% and 3.8±0.5% lower compared to both the C80 and R80 conditions, respectively, at a workrate of 30% LT power (both $p < 0.01$; Table 4.3; Figure 4.3). Crank angular velocity at the C78 condition was 3.2±0.7% and 3.3±0.4% lower compared to the C80 and R80 conditions, respectively, at a workrate of 60% LT power (both $p < 0.01$; Table 4.3; Figure 4.4). Crank angular velocity at the C78 condition was 2.5±0.8% and 2.1±0.4% lower compared to both the C80 and R80 conditions, respectively, at a workrate of 90% LT power (both $p < 0.05$; Table 4.3; Figure 4.5). Angular velocities produced during ankle extension for the C80 and C78 were 12.3±4.9% and 19.5±5.4% lower, respectively, compared to the R80 condition at the workrate of 60% LT power (both $p < 0.05$; Table 4.3; Figure 4.4). Repeated measures ANOVA also revealed a significant effect of workrate on angular velocities produced during knee and hip extension C80, R80, and C78, during whole leg extension phase (all $p < 0.05$; Table 4.3). Subsequent post hoc analyses indicated that angular velocities produced during knee and hip extension increased with increasing workrates of 30%, 60%, and 90% LT power (all $p < 0.05$; Table 4.3).

The repeated measures ANOVA revealed significant effect of pedal speed ($p < 0.01$; Table 4.3), with no significant workrate ($p > 0.05$) and no significant pedal speed × workrate interaction, on crank angular velocity, and angular velocity produced during ankle extension for the C80, O80, and C75, during whole leg extension phase. Subsequent post hoc analyses indicated crank angular velocity at the C75 condition was 6.7±0.6% and 6.8±0.5% lower compared to both the C80 and O80 conditions, respectively, at a workrate of 30% LT power (both $p < 0.01$; Table 4.3; Figure 4.3). Crank angular velocity at the C75 condition was 6.1±0.9% and 6.2±0.8% lower compared to both the C80 and O80 conditions, respectively, at a workrate of 60% LT power (both $p < 0.01$; Table 4.3; Figure 4.4). Crank angular velocity at the C75 condition was 6.4±0.8% and 6.2±0.6% lower compared to both the C80 and O80 conditions, respectively, at a workrate of 90% LT power (both $p < 0.01$; Table 4.3; Figure 4.5). Angular velocity produced during ankle extension for the C75 condition was 11.1±9.8% and 25.8±7.0% lower, respectively, compared to the C80 and O80 conditions at a workrate of 30% LT power (both $p < 0.01$; Table 4.3; Figure 4.3). Angular velocities produced during ankle extension for the C80 and C75 were 19.9±3.3% and 28.3±6.4% lower, respectively, compared to the O80 condition at the workrate of 60% LT power (both $p < 0.05$; Table 4.3; Figure 4.4).

The repeated measures ANOVA also revealed significant effect of pedal speed ($p < 0.01$; Table 4.3) and workrate ($p < 0.05$), with no significant pedal speed × workrate interaction, on angular velocities produced during knee and hip extension for the C80, O80, and C75, during the whole leg extension phase. Subsequent post hoc analyses indicated angular velocity produced during knee extension at the C75 condition was

9.9±1.6% and 8.0±0.5% lower compared to both the C80 and O80 conditions, respectively, at a workrate of 30% LT power (both $p < 0.01$; Table 4.3; Figure 4.3). Angular velocity produced during knee extension at the C75 condition was 9.1±1.4% and 8.62±1.4% lower compared to both the C80 and O80 conditions, respectively, at a workrate of 60% LT power (both $p < 0.01$; Table 4.3; Figure 4.4). Angular velocity produced during knee extension at the C75 condition was 8.8±2.3% and 5.6±1.7% lower compared to both the C80 and O80 conditions, respectively, at a workrate of 90% LT power (both $p < 0.05$; Table 4.3; Figure 4.5). Angular velocity produced during hip extension at the C75 condition was 7.8±2.2% and 4.5±1.5% lower compared to both the C80 and O80 conditions, respectively, at a workrate of 30% LT power (both $p < 0.05$; Table 4.3; Figure 4.3). Angular velocities produced during hip extension at both the O80 and C75 conditions were 7.7±1.8% and 5.2±2.0% lower, respectively, compared to the C80 condition at a workrate of 60% LT power (both $p < 0.05$; Table 4.3; Figure 4.4). Angular velocity produced during hip extension at the C75 condition was 9.1±2.7% and 5.5±1.3% lower compared to both the C80 and O80 conditions, respectively, at a workrate of 90% LT power (both $p < 0.01$; Table 4.3; Figure 4.5).

Repeated measures ANOVA also revealed a significant effect of workrate on angular velocities produced during knee and hip extension C80, O80, and C75 conditions for the whole pedal cycle (all $p < 0.05$; Table 4.3). Subsequent post hoc analyses indicated that angular velocities produced during knee and hip extension increased with increasing workrates of 30%, 60%, and 90% LT power (all $p < 0.05$).

Joint-specific Kinematics during ECC80 (Crank Angle of 27°–129°)

The repeated measures ANOVA indicated no significant effect of eccentricity ($p > 0.05$; Table 4.3) and workrate ($p > 0.05$), and no significant pedal speed × workrate interaction ($p > 0.05$), on angular velocity produced during ankle extension for the C80, R80, and O80 conditions, during ECC80. Repeated measures ANOVA revealed a significant effect of workrate on angular velocities produced during knee and hip extension (all $p < 0.05$). Subsequent post hoc analyses indicated angular velocities produced during knee and hip extension increased with increasing workrates of 30%, 60%, and 90% LT power (all $p < 0.05$).

The repeated measures ANOVA revealed significant effect of pedal speed ($p < 0.01$; Table 4.3), with no significant pedal speed × workrate interaction (all $p > 0.05$), on crank angular velocity, and angular velocities produced during knee and hip extension for the C80, R80, and O80 conditions. Subsequent post hoc analyses indicated that crank angular velocity at the O80 condition was 4.5±0.7% and 3.3±0.8% lower compared to both the C80 and R80 conditions, respectively, at a workrate of 30% LT power (both $p < 0.01$; Table 4.3; Figure 4.3). Crank angular velocity at the O80 condition was 4.6±0.5% and 3.0±0.6% lower compared to both the C80 and R80 conditions, respectively, at a workrate of 60% LT power (both $p < 0.01$; Table 4.3; Figure 4.4). Crank angular velocity at the R80 condition was 2.1±0.7% lower compared to both the C80 condition at a workrate of 90% LT power ($p < 0.05$; Table 4.3; Figure 4.5). In addition, crank angular velocity at the O80 condition was 4.8±0.6% and 2.7±0.3% lower compared to both the C80 and R80 conditions, respectively, at a workrate of 90% LT power (both $p < 0.01$; Table 4.3; Figure 4.5). Angular velocity produced during knee extension at the O80

condition was 7.2±2.1% lower compared to the C80 condition at a workrate of 30% LT power ($p < 0.05$). Angular velocities produced during knee extension at the R80 and O80 conditions were 3.9±1.7% and 8.1±1.6% lower, respectively, compared to the C80 condition at a workrate of 60% LT power ($p < 0.05$; Table 4.3; Figure 4.4). Angular velocity produced during knee extension at the O80 condition was 8.5±2.3% lower compared to the C80 condition at a workrate of 90% LT power ($p < 0.05$; Table 4.3; Figure 4.5). Angular velocity produced during hip extension at the O80 condition was 6.5±1.6% and 5.7±2.0% lower compared to both the C80 and R80 conditions, respectively, at a workrate of 30% LT power ($p < 0.05$; Table 4.3; Figure 4.3). Angular velocity produced during hip extension at the O80 condition was 7.1±2.0% lower compared to the C80 condition at a workrate of 60% LT power ($p < 0.01$; Table 4.3; Figure 4.4). Angular velocity produced during hip extension at the O80 condition was 6.4±2.4% lower compared to the C80 condition at a workrate of 90% LT power ($p < 0.05$; Table 4.3; Figure 4.5).

Repeated measures ANOVA revealed a significant effect of pedal speed ($p < 0.01$; Table 4.3), with no significant effect of workrate ($p > 0.05$) and no significant pedal speed × workrate interaction, on crank angular velocity for the C80, R80, and C78 during ECC80. Subsequent post hoc analyses indicated crank angular velocity at the C78 condition was 3.4±0.6% and 2.1±0.5% lower compared to both the C80 and R80 conditions, respectively, at a workrate of 30% LT power (both $p < 0.01$; Table 4.3; Figure 4.3). Crank angular velocity at the C78 condition was 3.3±0.7% and 1.7±0.4% lower compared to both the C80 and R80 conditions, respectively, at a workrate of 60% LT power (both $p < 0.01$; Table 4.3; Figure 4.4). Crank angular velocities at the R80 and

C78 conditions were 2.1±0.7% and 2.5±0.8% lower, respectively, compared to the C80 condition at a workrate of 90% LT power (both $p < 0.05$; Table 4.3; Figure 4.5). The repeated measures ANOVA also revealed a significant effect of workrate ($p < 0.05$; Table 4.3), with no significant effect of pedal speed (all $p > 0.05$) and no significant pedal × workrate interaction, on angular velocities produced during knee and hip extension during ECC80. Subsequent post hoc analyses indicated that angular velocities produced during knee and hip extension increased with increasing workrates of 30%, 60%, and 90% LT power (all $p < 0.05$).

Repeated measures ANOVA revealed a significant effect of pedal speed ($p < 0.01$; Table 4.3), with no significant effect of workrate ($p > 0.05$) and no significant pedal speed × workrate interaction, on crank angular velocity for the C80, O80, and C75 during ECC80. Subsequent post hoc analyses indicated crank angular velocities at the O80 and C78 conditions were 4.5±0.7% and 6.7±0.6% lower, respectively, compared to the C80 condition at a workrate of 30% LT power (both $p < 0.01$; Table 4.3; Figure 4.3). In addition, crank angular velocity at the C75 was 6.0±0.8% lower compared to the O80 condition at the workrate of 30 % LT power ($p < 0.05$; Table 4.3; Figure 4.3). Crank angular velocities at the O80 and C75 conditions were 4.6±0.5% and 6.1±0.9% lower, respectively, compared to the C80 condition at a workrate of 60% LT power (both $p < 0.01$; Table 4.3; Figure 4.4). Crank angular velocities at the O80 and C75 conditions were 4.8±0.6% and 6.5±0.8% lower, respectively, compared to the C80 condition at a workrate of 90% LT power (both $p < 0.01$; Table 4.3; Figure 4.5). In addition, crank angular velocity at the C75 was also 1.8±0.6% lower compared to the O80 condition at the workrate of 90 % LT power ($p < 0.05$; Table 4.3; Figure 4.5).

Repeated measures ANOVA also revealed a significant effect of pedal speed (all $p < 0.01$; Table 4.3) and workrate (all $p < 0.05$), with no significant pedal speed × workrate interaction (all $p > 0.05$), on angular velocities produced during knee and hip extension for the C80, O80, and C75, at workrates of 30%, 60%, and 90% LT power. Subsequent post hoc analyses indicated that angular velocities produced during knee extension at the O80 and C75 conditions were 7.2±2.1% and 9.8±1.3% lower, respectively, compared to the C80 condition at a workrate of 30% LT power (both $p < 0.01$; Table 4.3; Figure 4.3). In addition, angular velocity produced during knee extension at C75 was 2.8±0.7% lower compared to the O80 condition at the workrate of 30 % LT power ($p < 0.05$; Table 4.3; Figure 4.4). Angular velocities produced during knee extension at the O80 rpm and C75 conditions were 8.1±1.6% and 9.3±1.5% lower, respectively, compared to the C80 condition at a workrate of 60% LT power (both $p < 0.01$; Table 4.3; Figure 4.4). Angular velocities produced during knee extension at the O80 and C75 conditions were 8.5±2.3% and 9.4±2.4% lower, respectively, compared the C80 condition at a workrate of 90% LT power (both $p < 0.01$; Table 4.3; Figure 4.5). Angular velocities produced during hip extension at the O80 and C75 conditions were 6.5±1.6% and 7.4±2.0% lower, respectively, compared to the C80 condition at a workrate of 30% LT power (both $p < 0$ .01; Table 4.3; Figure 4.3). Angular velocities produced during hip extension at the O80 and C75 conditions were 7.1±2.0% and 7.8±1.8% lower, respectively, compared to the C80 condition at a workrate of 60% LT power (both $p < 0.01$; Table 4.3; Figure 4.4). Angular velocities produced during knee extension at the O80 and C75 conditions were 6.4±2.4% and 8.4±2.6% lower, respectively, compared to the C80 condition at a workrate of 90% LT power (both $p < 0.05$; Table 4.3; Figure 4.5).

Subsequent post hoc analyses also indicated that angular velocities produced during knee and hip extension increased with increasing workrates of 30%, 60%, and 90% LT power (all $p < 0.05$; Table 4.3).

Chainring Perception

Repeated measures ANOVA revealed no significant differences in chainring perception between the C, R, and O chainring conditions ($p = 0.74$). Participants achieved 50±19%, 38±18%, and 50±19% accuracy in chainring perception for the C, R, and O chainring conditions, respectively.

Discussion

A noncircular chainring's ability to manipulate crank angular velocity enables it to achieve slower pedal speed during the powerful leg extension phase compared to a circular chainring. Because pedal speed is a determinant of metabolic cost during submaximal cycling, a lower metabolic cost might be expected with a noncircular chainring compared to a circular chainring at the same pedaling rate. Although these strategies might potentially improve submaximal cycling performance, the main finding of this study was that cycling efficiency and metabolic cost during submaximal cycling did not differ significantly between circular and noncircular chainring conditions.

Cycling Efficiency and Metabolic Cost

Previous results for submaximal cycling performance with the use of noncircular chainrings have been mixed, with some investigators reporting improvements in

physiological responses (15, 32), while others detected no physiological effects between circular and noncircular chainrings (7, 18, 20, 33, 35). The lack of control of pedaling rate and/or pedal speed may explain these mixed findings. The decrease in pedal speed is the result of the noncircular chainring slowing down the crank angular velocity during the leg extension phase. Hence, the physiological improvements associated with the use of noncircular chainrings may be due to a pedal speed effect when pedaling rates are matched between circular and noncircular chainrings. An important part of my experimental design in this study was the decoupling of pedal speed from chainring shape/eccentricity by evaluating cycling efficiency and metabolic cost with the use of a noncircular chainring and a circular chainring matched for pedal speed during leg extension. As expected, GE and metabolic cost did not differ between a noncircular and circular chainring condition matched for pedal speed. Similarly, GE and metabolic cost also did not differ between circular and noncircular chainring conditions at matched pedaling rates. This could suggest that the eccentricities (1.13 and 1.24) of the commercially available noncircular chainrings utilized in this study might not be large enough to allow us to measurably detect physiological improvements. Interestingly, Hull and colleagues (20) evaluated physiological responses to cycling utilizing a noncircular chainring of eccentricity 1.36, and reported no improvements in GE compared to a circular chainring. Despite this large eccentricity, these authors acknowledged that the lack in control of pedaling rate might have confounded the results of the study. Nevertheless, the results of this present study support previous reports (18, 20, 35) that noncircular chainrings do not offer any advantage in submaximal cycling performance over circular chainrings.

Additionally, the range of pedaling rates (3–5 rpm accounting for a 2–5% variation in pedal speed) utilized in this present study may not be sufficient to measurably influence metabolic cost and cycling efficiency. McDaniel and colleagues (30) demonstrated that pedal speed accounted for an additional 3% variation in metabolic cost above the 95% accounted for by power. This observation was based on a large (> 3 fold) range of pedal speeds (0.6–2.0 m/s). In contrast, the small (3–5 rpm) differences imposed by the noncircular chainrings are simply trivial (0.85–0.88 m/s or a 4% variation), and thus would not be expected to produce any measurable effect.

My findings do not support manufacturers' claims of increased power or efficiency. One possible explanation for this conflict could be due to the approach to which power is calculated by some commercial powermeters. For example, Schoberer Rad Messtechnik (SRM) powermeters calculate power by multiplying average torque for each crank revolution with average crank angular velocity, from torque data collected at 200Hz. This approach inflates power because noncircular chainrings spend more time within the high torque portion of the pedal cycle. To illustrate this effect, we calculated power by multiplying average torque from our pedal force with average crank angular velocity. Values calculated with this approach (similar to a SRM powermeter) were inflated by 2.7% compared to the approach of averaging instantaneous power. Thus, cyclists may be misled by their own powermeters into believing that they are achieving higher power and subsequently greater cycling efficiency with the use of noncircular chainrings.

Joint-specific Kinematics

To the best of my knowledge, this is the only study to have evaluated the influence of noncircular chainrings on joint-specific kinematics and kinetics during submaximal cycling. The results of this study indicated that knee and hip angular velocities were significantly reduced, while ankle angular velocity remained unaffected with the use of the noncircular charining. These results were unanticipated, as I was expecting the noncircular chainring's ability to manipulate joint angular velocity would be negated by the redundant DOF at the ankle during submaximal cycling. The results from this present study also contrasted those from study two, suggesting that the noncircular chainrings affected the more powerful knee and hip extension actions during submaximal cycling. These comparisons demonstrate that alterations in joint-specific kinematics may reflect differences in the task/goal of producing and controlling a target power during submaximal cycling versus maximizing power during maximal cycling (14, 24). Indeed, Elmer and colleagues (14) reported increasing duty cycle (portions of cycle spent in extension) values transitioning from submaximal to maximal cycling. While the results from this present study may suggest that the noncircular chainrings were able to affect joint-specific angular velocity, a similar effect was also achieved with the use of a circular chainring matched to the pedal speed of a noncircular chainring. This further supports the need to control for pedaling rate and/or pedal speed when evaluating the influence of noncircular chainings on physiological responses. Despite the alterations in joint-specific kinematics, the eccentricities and/or pedal speeds utilized in this investigation did not improve cycling efficiency or metabolic cost during submaximal cycling. Although, it is plausible that the eccentricities and/or pedal speeds utilized in

this investigation were not sufficiently large enough to affect submaximal cycling performance, it may also imply that cycling efficiency and metabolic cost associated with the use of the noncircular chainrings is similar to that associated with the use of conventional circular chainrings.

Summary

This is the first investigation to evaluate physiological responses and joint-specific kinematics involving the use of noncircular chainrings during submaximal cycling. In addition, I was also the first to account for eccentricity mimicking a lower pedal speed in our experimental design. Despite the noncircular chainrings imposing their eccentricity on joint angular kinematics, the lack of improvement in physiological responses together with metabolic cost and GE, suggest that noncircular chainrings do not provide a performance benefit during steady-state efforts of submaximal intensity. Nevertheless, I cannot exclude the possibility that a noncircular chainring of eccentricity larger that those commercially available, may result in improvements during submaximal cycling. Thus, future research that combines the evaluation of chainring eccentricities beyond those commercially available, with the experimental design of matching pedal speed, may help to determine the efficacy of noncircular chainrings on submaximal cycling performance.

Table 4.1: Study 3 participant descriptive characteristics (n = 8).

	Mean±SD
Age (yr)	35±8
Mass (kg)	75±7
Height (m)	1.77±0.07
$\dot{V}O_{peak}$ (ml/kg/min)	52±4
LT (% $\dot{V}O_{peak}$)	75±13
LT power (W)	244±56
30% LT power (W)	73±17
60% LT power (W)	146±34
90% LT power (W)	219±51

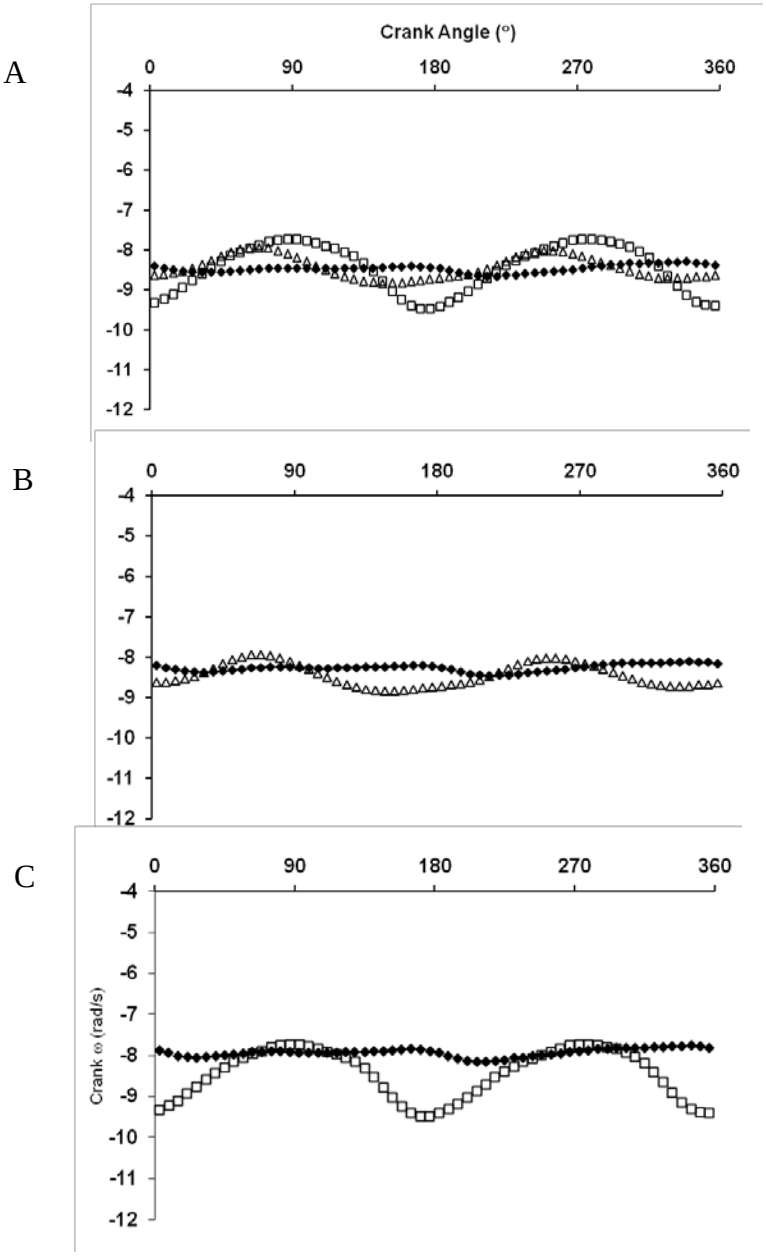

Figure 4.1: Crank angular velocity profiles of the C (◆), R (Δ), and O (□) chainring conditions at the workrate of 90% LT power (representative of 30% and 60% LT power). Crank angles of 0° and 360° represent the top dead center position, and 180° represents the bottom dead center position. Crank angular velocity profiles of the C80, R80, and O80 conditions (A). Crank angular velocity profiles of R80 and C78 (matched for R80 pedal speed of 0.88 m/s) conditions (B). Crank angular velocity profiles of O80 and C75 (matched for O80 pedal speed of 0.85 m/s) (C).

Table 4.2. Physiological responses to steady-state submaximal cycling trials at workrates of 30%, 60%, and 90% LT power. Data presented as mean±SEM.

	C80	Matched Pedal Speed		Matched Pedal Speed	
		R80	C78	O80	C75
30% LT					
$\dot{V}O_2$ (L /min) [a]	1.38±0.06	1.37±0.06	1.35±0.05	1.37±0.05	1.39±0.06
RER	0.87±0.02	0.89±0.02	0.86±0.02	0.85±0.02	0.81±0.02
Metabolic Cost (kcal/h) [a]	400±17	400±16	394±17	402±15	395±16
GE (%)[a]	15.8±1.1	15.8±1.0	16.0±1.0	15.7±1.1	15.9±1.0
HR (beats/min) [a]	103±3	103±3	103±1	103±2	105±3
$RPE_{overall}$ [a]	9±1	8±1	8±1	9±1	9±1
RPE_{legs} [a]	8±1	8±1	8±1	9±1	8±1
60% LT					
$\dot{V}O_2$ (L /min) [a]	2.17±0.10	2.12±0.10	2.11±0.10	2.14±0.10	2.16±0.10
RER [a]	0.88±0.02	0.90±0.01	0.89±0.01	0.88±0.01	0.87±0.02
Metabolic Cost (kcal/h) [a]	636±27	625±30	623±31	627±28	623±28
GE (%)[a]	19.8±1.2	20.1±1.2	20.2±1.2	20.0±1.2	20.2±1.2
HR (beats/min) [a]	125±4	124±4	126±3	123±3	124±4
$RPE_{overall}$ [a]	12±1	11±1	11±1	11±1	11±1
RPE_{legs} [a]	12±1	11±1	12±1	11±1	11±1
90% LT					
$\dot{V}O_2$ (L /min) [a]	2.94±0.14	2.96±0.16	2.95±0.15	2.97±0.15	2.98±0.15
RER [a]	0.96±0.01	0.98±0.01	0.96±0.01	0.96±0.01	0.98±0.01
Metabolic Cost (kcal/h) [a]	882±41	890±48	886±47	891±45	891±43
GE (%)[a]	21.5±1.3	21.2±1.2	21.3±1.2	21.1±1.2	21.2±1.3
HR (beats/min) [a]	147±5	149±5	151±5	147±3	148±4
$RPE_{overall}$ [a]	14±1	14±1	14±1	14±1	14±1
RPE_{legs} [a]	15±1	14±1	15±1	15±1	15±1

[a] Main effect of workrate ($p < 0.01$).

A

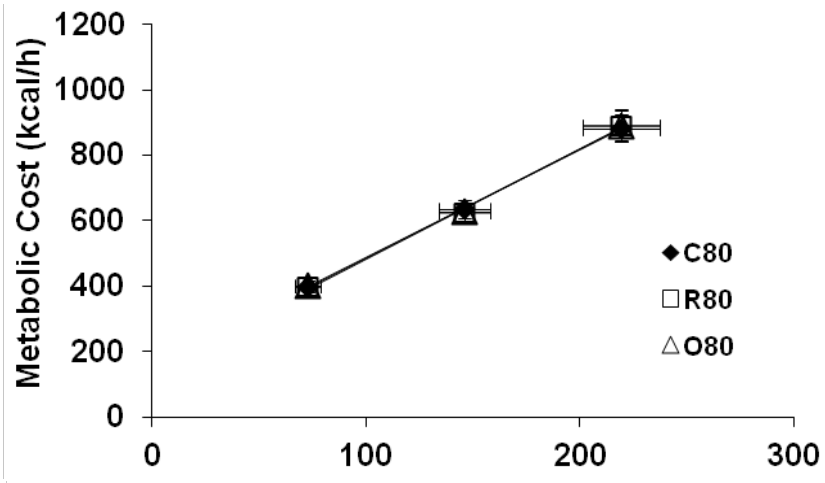

B

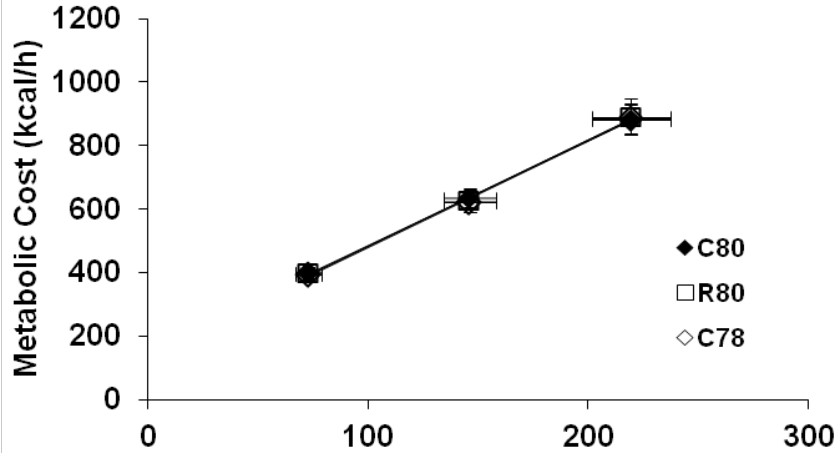

C

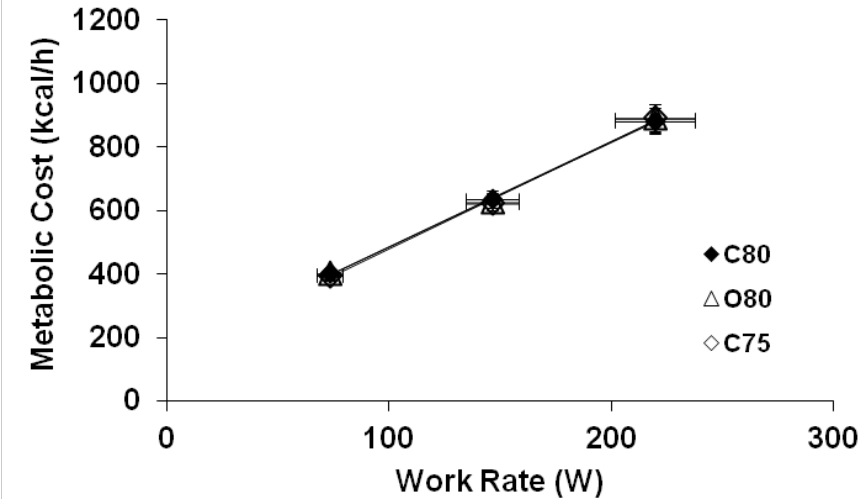

Figure 4.2: Metabolic cost as a function of work rate. Metabolic cost did not differ significantly between C80, R80, O80, C75, and C78 conditions.

Table 4.3. Joint-specific angular velocity produced during the whole leg extension phase and ECC 80 (crank angle of 27°–129°) for C80, R80, O80, C75, and C78 conditions at workrates of 30%, 60%, and 90% LT power. Data presented as mean±SEM.

Angular Velocity (rad/s)	C80	Matched Pedal Speed		Matched Pedal Speed	
		R80	C78	O80	C75
(30% LT power) Whole Leg Extension Phase					
Crank	–8.45±0.04	–8.49±0.04	–8.17±0.02$^{*,\#}$	–8.46±0.06	–7.88±0.04*,†
Ankle Extension	–0.92±0.14	–1.00±0.09	–0.75±0.11	–1.03±0.07	–0.77±0.10*
Knee Extension^{b}	3.41±0.08	3.39±0.05	3.26±0.06	3.33±0.06	3.07±0.05*,†
Hip Extension^{b}	–2.28±0.05	–2.29±0.04	–2.23±0.04	–2.20±0.05	–2.10±0.06*,†
ECC80					
Crank^{a}	–8.48±0.04	–8.37±0.04	–8.19±0.02$^{*,\#}$	–8.09±0.06$^{*,\#}$	–7.91±0.04*,†
Ankle Extension	–0.77±0.23	–0.65±0.08	–0.56±0.12	–0.61±0.15	–0.51±0.17
Knee Extension^{a,b}	4.34±0.12	4.21±0.08	4.14±0.08	4.02±0.08*	3.91±0.04*,†
Hip Extension^{a,b}	–2.84±0.07	–2.81±0.03	–2.77±0.04	–2.65±0.06$^{*,\#}$	–2.62±0.08*
(60% LT power) Whole Leg Extension Phase					
Crank	–8.46±0.05	–8.47±0.03	–8.19±0.03$^{*,\#}$	–8.47±0.03	–7.95±0.05*,†
Ankle Extension	–0.91±0.15	–1.05±0.16	–0.82±0.12$^{\#}$	–1.11±0.16	–0.81±0.13†
Knee Extension^{b}	3.54±0.08	3.49±0.09	3.42±0.07	3.44±0.06	3.21±0.07*,†
Hip Extension^{b}	–2.39±0.07	–2.33±0.08	–2.34±0.05	–2.26±0.06*	–2.20±0.07*
ECC80					
Crank^{a}	–8.49±0.05	–8.35±0.04	–8.21±0.03$^{*,\#}$	–8.10±0.03*	–7.97±0.05*
Ankle Extension	–0.58±0.23	–0.68±0.20	–0.44±0.14	–0.50±0.15	–0.46±0.17
Knee Extension^{a,b}	4.50±0.11	4.32±0.12*	4.34±0.10	4.13±0.08*	4.07±0.09*
Hip Extension^{a,b}	–2.96±0.09	–2.87±0.08	–2.91±0.04	–2.74±0.06*	–2.73±0.05*
(90% LT power) Whole Leg Extension Phase					
Crank	–8.48±0.06	–8.44±0.03	–8.19±0.03$^{*,\#}$	–8.46±0.04	–7.93±0.04*,†
Ankle Extension	–0.98±0.19	–1.05±0.16	–0.82±0.12$^{\#}$	–1.01±0.08	–0.80±0.11
Knee Extension^{b}	3.67±0.11	3.62±0.08	3.42±0.07	3.53±0.06	3.33±0.08*,†
Hip Extension^{b}	–2.46±0.09	–2.40±0.09	–2.34±0.05	–2.36±0.07	–2.23±0.08*,†
ECC80					
Crank^{a}	–8.50±0.06	–8.32±0.03*	–8.21±0.03$^{*,\#}$	–8.09±0.04$^{*,\#}$	–7.94±0.04*,†
Ankle Extension	–0.61±0.36	–0.57±0.19	–0.44±0.14	–0.30±0.14	–0.48±0.15
Knee Extension^{a,b}	4.67±0.15	4.47±0.11	4.34±0.10	4.25±0.09*	4.21±0.11*
Hip Extension^{a,b}	–3.04±0.10	–2.96±0.08	–2.91±0.04	–2.84±0.08*	–2.78±0.09*

Significantly lower than C condition ($p < 0.05$).

$^{\#}$ Significantly lower than R condition ($p < 0.05$).

†Significantly lower than O condition ($p < 0.05$).

^{a} Main effect of pedal speed ($p < 0.01$).

^{b} Main effect of workrate ($p < 0.05$).

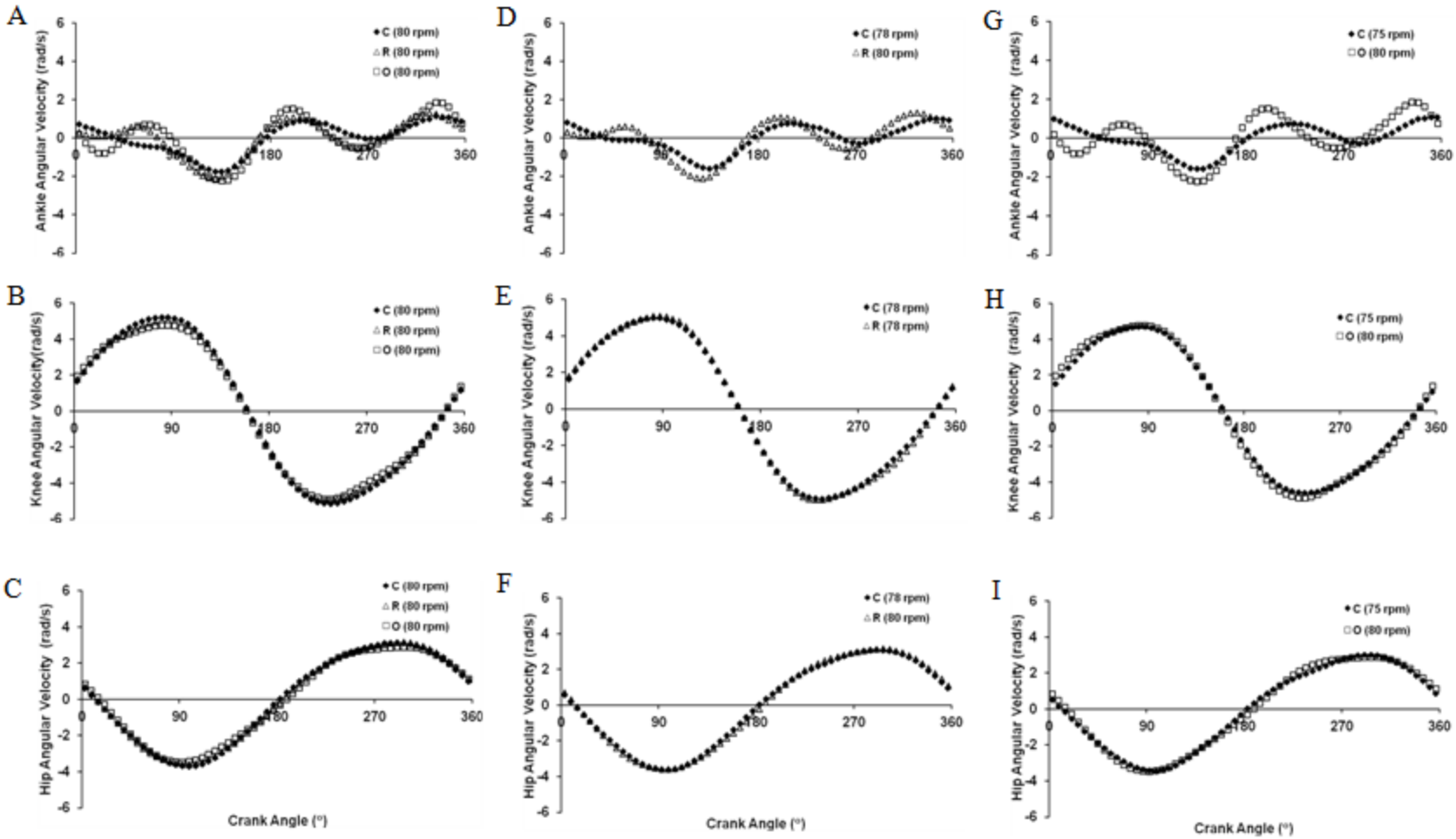

Figure 4.3: Joint-specific kinematics versus crank angle during submaximal cycling at workrate of 30% LT power. Mean angular velocities produced by: ankle (A), knee (B), and hip (C) joint actions for C (80 rpm), R (80 rpm), and O (80 rpm); ankle (D), knee (E), and hip (F) joint actions for R (80 rpm) and C (78 rpm); ankle (G), knee (H), and hip (I) joint actions for O (80 rpm) and C (75 rpm). Crank angles of 0° and 360° represent the top dead center position, and 180° represents the bottom dead center position.

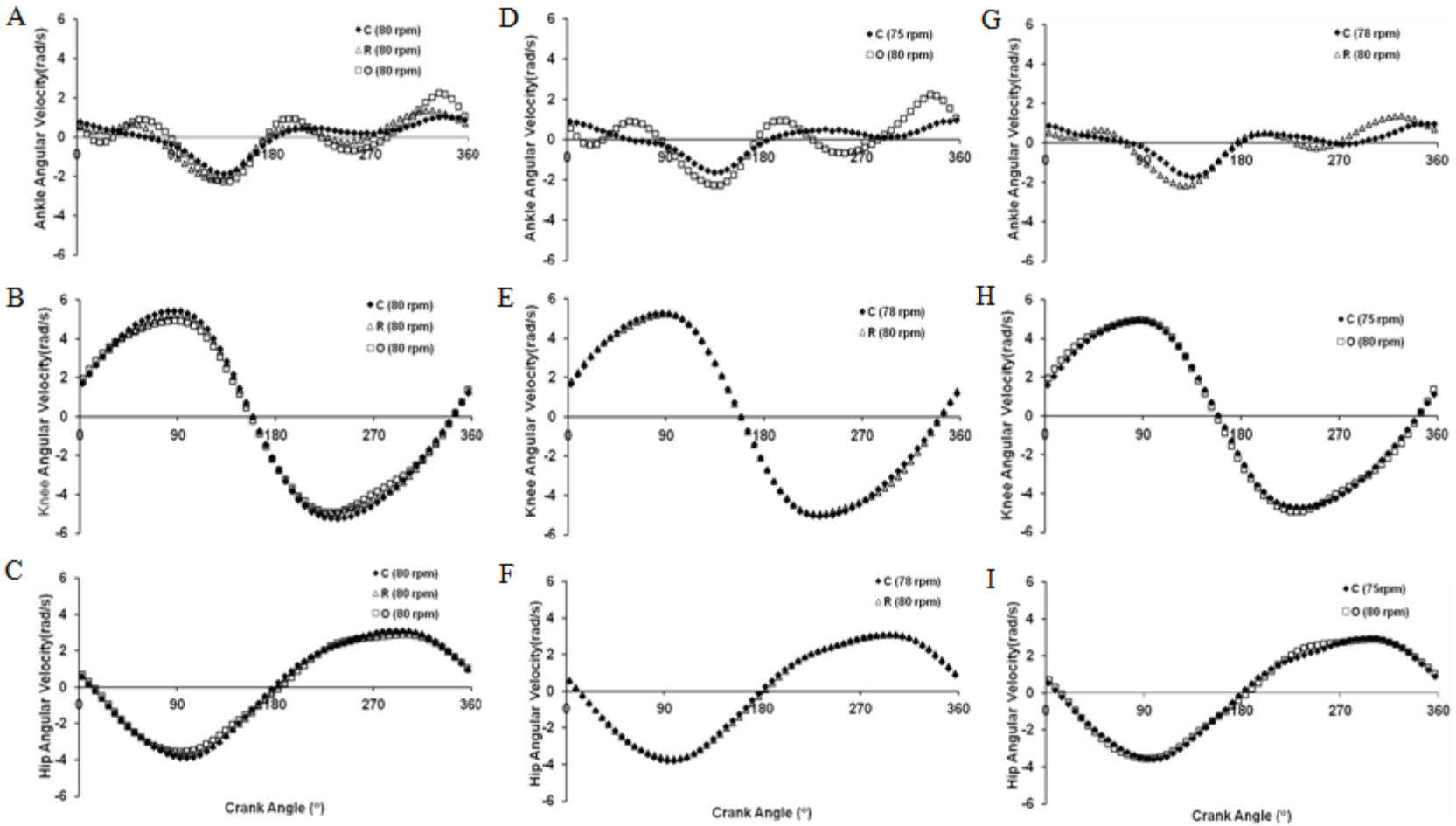

Figure 4.4: Joint-specific kinematics versus crank angle during submaximal cycling at workrate of 60% LT power. Mean angular velocities produced by: ankle (A), knee (B), and hip (C) joint actions for C (80 rpm), R (80 rpm), and O (80 rpm); ankle (D), knee (E), and hip (F) joint actions for R (80 rpm) and C (78 rpm); ankle (G), knee (H), and hip (I) joint actions for O (80 rpm) and C (75 rpm). Crank angles of 0° and 360° represent the top dead center position, and 180° represents the bottom dead center position.

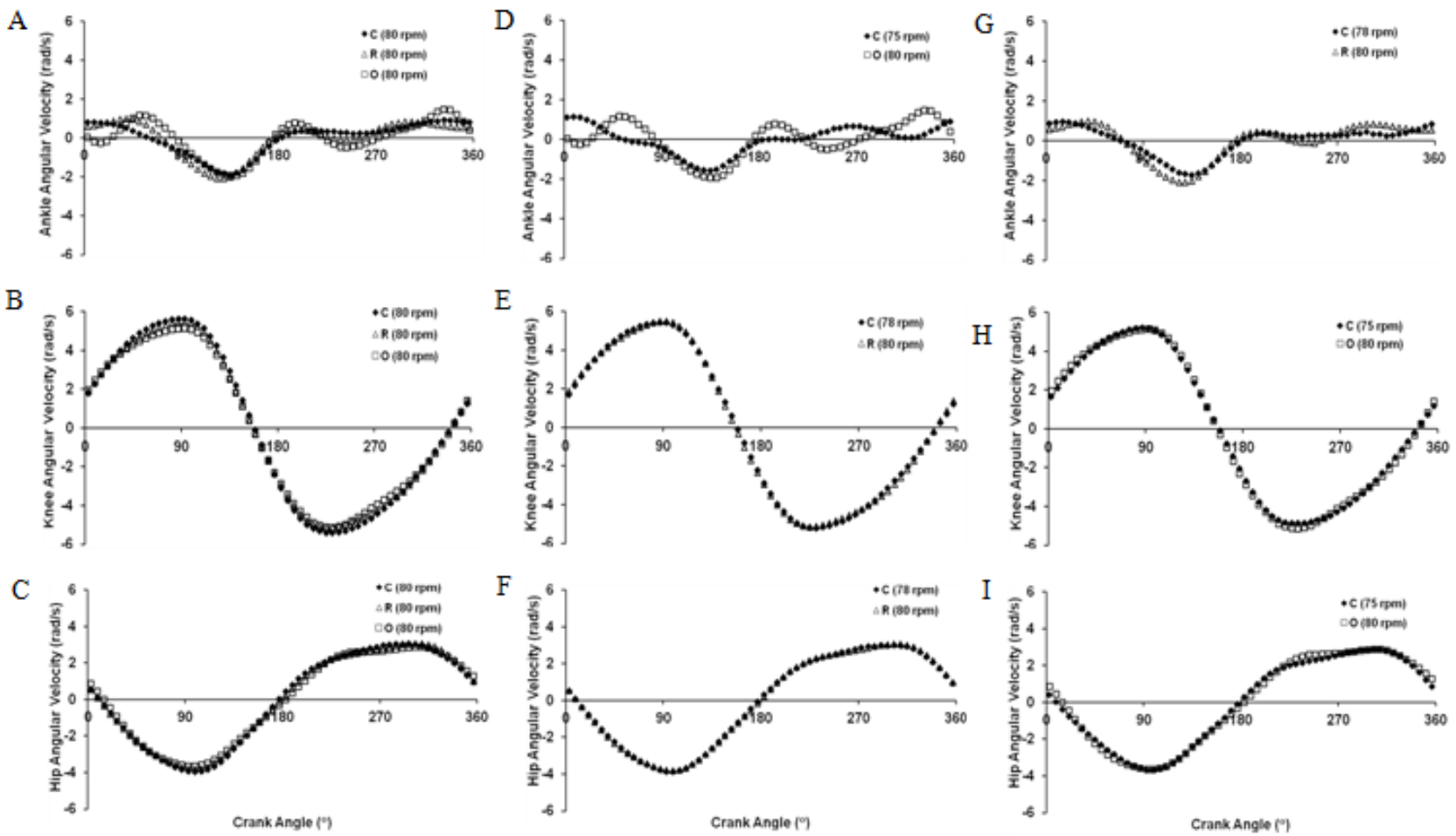

Figure 4.5: Joint-specific kinematics versus crank angle during submaximal cycling at workrate of 90% LT power. Mean angular velocities produced by: ankle (A), knee (B), and hip (C) joint actions for C (80 rpm), R (80 rpm), and O (80 rpm); ankle (D), knee (E), and hip (F) joint actions for R (80 rpm) and C (78 rpm); ankle (G), knee (H), and hip (I) joint actions for O (80 rpm) and C (75 rpm). Crank angles of 0° and 360° represent the top dead center position, and 180° represents the bottom dead center position.

CHAPTER 5

SUMMARY, IMPLICATIONS, AND RECOMMENDATIONS

Summary

In this series of studies, I evaluated the influence of noncircular chainrings on maximal and submaximal cycling performance. Commercial noncircular chainrings (e.g., Rotor, Osymetric) are designed to increase the time spent in extension and flexion, and decrease the time spent in the transition phases. Previous comparisons of circular and noncircular chainrings have produced positive (32, 34) and negative findings (7, 33). Firstly, these mixed findings may be due to participants cycling at lower pedal speeds (marker for muscle shortening velocity) with the noncircular chainrings, contributing to increase power production when pedaling rates are matched. Secondly, it may also be related to differences in power-pedaling rate relationships when pedaling rates were self-selected. Hence, in the first study I evaluated the influence of noncircular chainrings on maximum cycling power and optimal pedaling rate. The main finding of the first study was that chainring eccentricity did not influence maximum cycling power and optimal pedaling rate. In addition, I also observed a trend of decreasing power with increasing chainring eccentricity at high pedaling rates. These results suggest that multiple degrees of freedom in the leg, crank, and pedal system may allow the manipulation of joint angular velocity in such a way as to negate the effects of the noncircular chainrings.

Consequently, in the second study I evaluated the influence of noncircular chainrings joint-specific kinematics and power production during maximal cycling at a range of pedaling rates (60, 90, and 120 rpm). The results indicated that chainring eccentricity did not influence joint-specific power production during maximal cycling. Further, a novel finding in the second study was that despite the noncircular chainring's ability to manipulate crank angular velocity, only ankle angular velocity was affected, while knee and hip angular velocities remained unaffected. This suggests that cyclists were able to defend and preserve their knee and hip joint actions as the dominant power-producing actions, by affording the redundant DOF at the ankle against perturbations at the crank. In the third study, I evaluated the influence of noncircular chainrings on physiological responses during submaximal cycling. To the best of my knowledge, this is the first study to control for pedal speed by taking into account that eccentricity mimics a lower pedal speed. This is an important consideration because pedal speed is a determinant of the metabolic cost during submaximal cycling (30). The main finding of the third study was that chainring eccentricity did not influence physiological responses, metabolic cost, and cycling efficiency during submaximal cycling. Taken together, these findings indicate that despite the sound theories associated with the noncircular chainrings, they do not offer an advantage over a conventional circular chainring during maximal and submaximal cycling in trained cyclists.

Implications

Our findings related to the noncircular chainring influencing the power-pedaling rate relationship at high pedaling rates may have practical implications for coaches and

athletes. Specifically, an increase in chainring eccentricity elicited greater reduction in cycling power at 150 rpm. Hence, noncircular chainrings may negatively affect power production for athletes who participate in cycling events eliciting high pedaling rates (≥ 150 rpm). Conversely, noncircular chainrings did not influence joint-specific power production at pedaling rates 60, 90, and 120 rpm during maximal cycling due to the cyclists adopting a strategy exploiting redundant DOF at the ankle joint. Thus, noncircular chainrings offer neither an advantage nor disadvantage over a conventional circular chainring during maximal cycling at pedaling rates ranging from 60 – 120 rpm. Finally, the noncircular chainrings also did not measurably improve submaximal cycling performance. Indeed, I observed a 2 % variation in cycling efficiency and metabolic cost between the circular and noncircular chainrings. Similarly, these results suggest that noncircular chainrings neither improve nor compromise submaximal cycling performance in trained cyclists.

Future Recommendations

Overall, the results from these series of studies provide interesting information to researchers and athletes regarding the use of noncircular chainrings during maximal and submaximal cycling. Our findings have also produced directions for future research. A limitation in the first study was the speculation that the negative results of reduced cycling power at 150 rpm with the use of the noncircular chainrings could be due to reduced time for muscle excitation and relaxation within the transition phases offsetting the intended gains of spending more time in the power producing phases. The use of electromyography (EMG) would allow the quantification of changes in both level and

timing aspects of muscular activation of the lower limb muscles with the use of a noncircular chainring during maximal cycling. These EMG measures could similarly be extended to investigate the alteration of muscle coordination during submaximal cycling. It is important to note that the eccentricities of the commercially available chainrings utilized in these series of studies may not be sufficient to elicit measureable improvements in maximal and submaximal cycling performance. A future direction would be to combine the methodological approaches used in these series of studies with the utilization of chainring eccentricities beyond those commercially available (20, 34).

REFERENCES

1. Beedie, C.J., and A.J. Foad. The placebo effect in sports performance: a brief review. *Sports Med.* 39:313-29, 2009.

2. Beedie, C.J., A.J. Foad, and D.A. Coleman. Identification of placebo responsive participants in 40km laboratory cycling performance. *J Sports Sci Med.* 7:166-75, 2008.

3. Beedie, C.J., et al. Placebo effects of caffeine on cycling performance. *Med Sci Sports Exerc.* 38:2159-64, 2006.

4. Caiozzo, V.J., and K.M. Baldwin. Determinants of work produced by skeletal muscle: potential limitations of activation and relaxation. *Am J Physiol.* 273:C1049-56, 1997.

5. Chavarren, J., and J.A. Calbet. Cycling efficiency and pedalling frequency in road cyclists. *Eur J Appl Physiol Occup Physiol.* 80:555-63, 1999.

6. Clark, V.R., et al. Placebo effect of carbohydrate feedings during a 40-km cycling time trial. *Med Sci Sports Exerc.* 32:1642-7, 2000.

7. Cordova, A., et al. Physiological responses during cycling with oval chainrings (Q-Ring) and circular chainrings. *J Sports Sci Med.* 13:410-6, 2014.

8. Coyle, E.F. Physiological determinants of endurance exercise performance. *J Sci Med Sport.* 2:181-9, 1999.

9. Coyle, E.F., et al. Cycling efficiency is related to the percentage of type I muscle fibers. *Med Sci Sports Exerc.* 24:782-8, 1992.

10. Cullen, L.K., et al. Efficiency of trained cyclists using circular and noncircular chainrings. *Int J Sports Med.* 13:264-9, 1992.

11. de Leva, P. Adjustments to Zatsiorsky-Seluyanov's segment inertia parameters. *J Biomech.* 29:1223-30, 1996.

12. Dorel, S., et al. Adjustment of muscle coordination during an all-out sprint cycling task. *Med Sci Sports Exerc.* 44:2154-64, 2012.

13. Elftman, H. Forces and energy changes in the leg during walking. *Am J Phys-Leg Cont.* 125:339-356, 1939.

14. Elmer, S.J., et al. Joint-specific power production during submaximal and maximal cycling. *Med Sci Sports Exerc.* 43:1940-7, 2011.

15. Hansen, E.A., et al. Effect of chain wheel shape on crank torque, freely chosen pedal rate, and physiological responses during submaximal cycling. *J Physiol Anthropol.* 28:261-7, 2009.16. Harrison, J.Y. Maximizing human power output by suitable selection of motion cycle and load. *Hum Factors.* 12:315-329, 1970.

17. Hopkins, W.G. Measures of reliability in sports medicine and science. *Sports Med.* 30:1-15, 2000.

18. Horvais, N., et al. Effects of a noncircular chainring on muscular, mechanical and physiological parameters during cycle ergometer tests. *Isokinetics and Exercise Science.* 15:271-279, 2007.

19. Hue, O., et al. Enhancing cycling performance using an eccentric chainring. *Med Sci Sports Exerc.* 33:1006-10, 2001.

20. Hull, M.L., et al. Physiological response to cycling with both circular and noncircular chainrings. *Med Sci Sports Exerc.* 24:1114-22, 1992.

21. Kalasountas, V., J. Reed, and J. Fitzpatrick. The effect of placebo-induced changes in expectancies on maximal force production in college students. *J Appl Sport Psychol.* 19:116-124, 2007.

22. Kautz, S.A., and M.L. Hull. A theoretical basis for interpreting the force applied to the pedal in cycling. *J Biomech.* 26:155-65, 1993.

23. Martin, J.C. Muscle power: the interaction of cycle frequency and shortening velocity. *Exerc Sport Sci Rev.* 35:74-81, 2007.

24. Martin, J.C., and N.A. Brown. Joint-specific power production and fatigue during maximal cycling. *J Biomech.* 42:474-9, 2009.

25. Martin, J.C., et al. A governing relationship for repetitive muscular contraction. *J Biomech.* 33:969-74, 2000.

26. Martin, J.C., D. Diedrich, and E.F. Coyle. Time course of learning to produce maximum cycling power. *Int J Sports Med.* 21:485-7, 2000.

27. Martin, J.C., et al. A low-cost instrumented spatial linkage accurately determines ASIS position during cycle ergometry. *J Appl Biomech.* 23:224-9, 2007.

28. Martin, J.C., S.M. Lamb, and N.A. Brown. Pedal trajectory alters maximal single-leg cycling power. *Med Sci Sports Exerc.* 34:1332-6, 2002.

29. Martin, J.C., B.M. Wagner, and E.F. Coyle. Inertial-load method determines maximal cycling power in a single exercise bout. *Med Sci Sports Exerc.* 29:1505-12, 1997.

30. McDaniel, J., et al. Determinants of metabolic cost during submaximal cycling. *J Appl Physiol.* 93:823-8, 2002.

31. Neptune, R.R., and M.L. Hull. Accuracy assessment of methods for determining hip movement in seated cycling. *J Biomech.* 28:423-37, 1995.

32. O'Hara, C.R., et al. Effects of chainring type (Circular vs. Rotor Q-Ring) on 1km time trial performance over six weeks in competitive cyclists and triathletes. *Int J Sports Sci Eng.* 6:25-40, 2012.

33. Peiffer, J.J., and C.R. Abbiss. The influence of elliptical chainrings on 10 km cycling time trial performance. *Int J Sports Physiol Perform.* 5:459-68, 2010.

34. Rankin, J.W., and R.R. Neptune. A theoretical analysis of an optimal chainring shape to maximize crank power during isokinetic pedaling. *J Biomech.* 41:1494-502, 2008.

35. Ratel, S., et al. Physiological responses during cycling with noncircular "Harmonic" and circular chainrings. *Eur J Appl Physiol.* 91:100-4, 2004.

36. Santalla, A., et al. A new pedaling design: the Rotor--effects on cycling performance. *Med Sci Sports Exerc.* 34:1854-8, 2002.

37. Shan, G. Biomechanical evaluation of bike power saver. *Appl Ergon.* 39:37-45, 2008.

38. Tanner, R.K., and C.J. Gore. *Physiological tests for elite athletes*. Champaign: Human Kinetics, 2012, pp. 546.

39. Woltring, H.J. A Fortran package for generalized, cross-validatory spline smoothing and differentiation. *Adv Eng Softw.* 8:104-113, 1986.

40. Yoshihuku, Y., and W. Herzog. Optimal design parameters of the bicycle-rider system for maximal muscle power output. *J Biomech.* 23:1069-79, 1990.

41. Zuntz, N. uber die Bedeutung der verschiedene Nahrstoffe als Erzeuber der Muskelkraft. *Pflugers Arch.* 83:557-571, 1901.